iScience

CellPress
OPEN ACCESS

Article

The deubiquitinase Otud7b suppresses cone photoreceptor degeneration in mouse models of retinal degenerative diseases

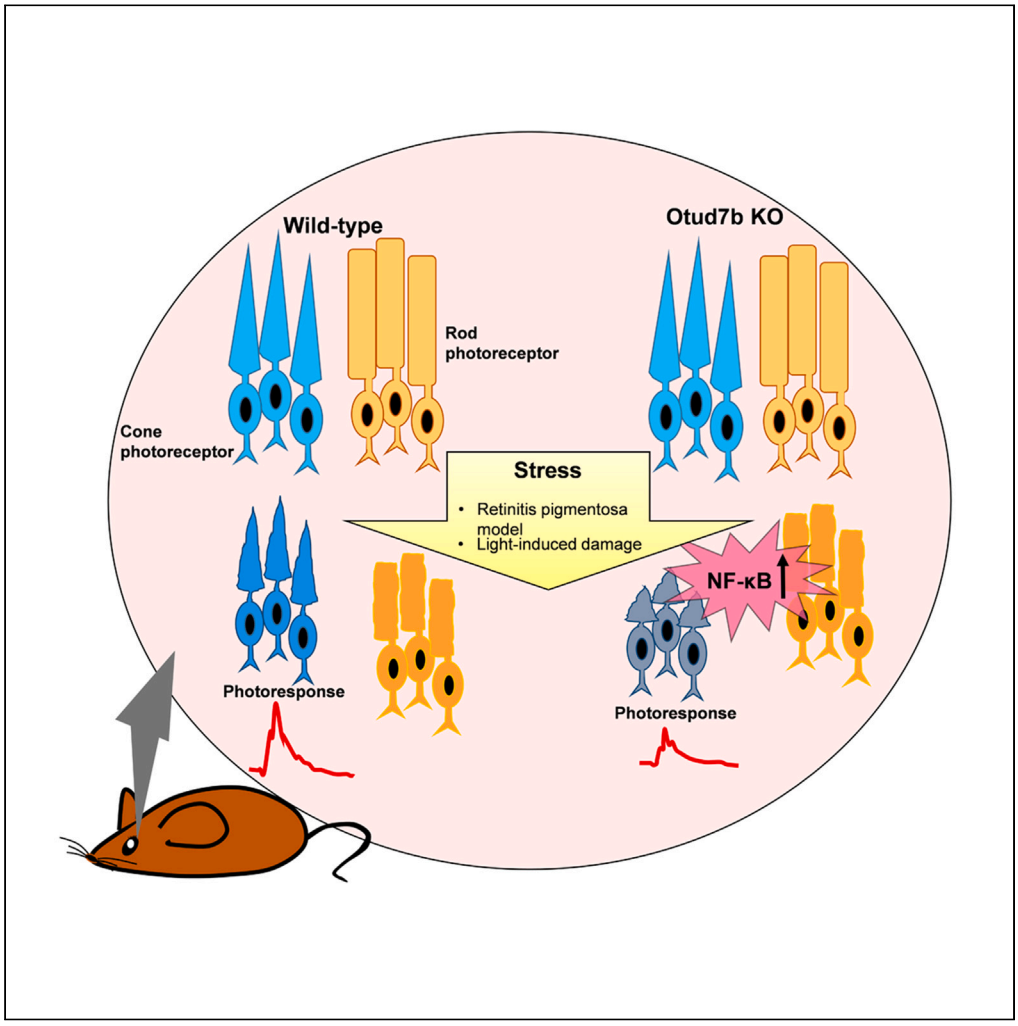

Leah Rie Varner, Taro Chaya, Yamato Maeda, ..., Toshinori Tsujii, Daisuke Okuzaki, Takahisa Furukawa

taro.chaya@protein.osaka-u.ac.jp (T.C.)
takahisa.furukawa@protein.osaka-u.ac.jp (T.F.)

Highlights

Cone photoreceptor damage by light exposure stress is increased in *Otud7b*$^{-/-}$ mice

Otud7b deficiency exacerbates cone degeneration in retinitis pigmentosa mouse model

NF-κB is activated in photoreceptor cells of the light-exposed *Otud7b*$^{-/-}$ retina

NF-κB inhibition attenuates cone damage in the light-exposed *Otud7b*$^{-/-}$ retina

Varner et al., iScience 27, 109380
April 19, 2024
https://doi.org/10.1016/j.isci.2024.109380

iScience

CellPress
OPEN ACCESS

Article

The deubiquitinase Otud7b suppresses cone photoreceptor degeneration in mouse models of retinal degenerative diseases

Leah Rie Varner,[1] Taro Chaya,[1,*] Yamato Maeda,[1] Ryotaro Tsutsumi,[1] Shanshan Zhou,[1] Toshinori Tsujii,[1] Daisuke Okuzaki,[2] and Takahisa Furukawa[1,3,*]

SUMMARY

Primary and secondary cone photoreceptor death in retinal degenerative diseases, including age-related macular degeneration (AMD) and retinitis pigmentosa (RP), leads to severe visual impairment and blindness. Although the cone photoreceptor protection in retinal degenerative diseases is crucial for maintaining vision, the underlying molecular mechanisms are unclear. Here, we found that the deubiquitinase Otud7b/Cezanne is predominantly expressed in photoreceptor cells in the retina. We analyzed *Otud7b*$^{-/-}$ mice, which were subjected to light-induced damage, a dry AMD model, or were mated with an RP mouse model, and observed increased cone photoreceptor degeneration. Using RNA-sequencing and bioinformatics analysis followed by a luciferase reporter assay, we found that Otud7b downregulates NF-κB activity. Furthermore, inhibition of NF-κB attenuated cone photoreceptor degeneration in the light-exposed *Otud7b*$^{-/-}$ retina and stress-induced neuronal cell death resulting from *Otud7b* deficiency. Together, our findings suggest that Otud7b protects cone photoreceptors in retinal degenerative diseases by modulating NF-κB activity.

INTRODUCTION

Retinal photoreceptor cells are specialized neurons that perceive light and convert it into electrical signals that are transmitted to retinal ganglion cells, which send signals through the optic nerve to the brain. Photoreceptor cells in the vertebrate retina can be categorized into rods and cones. Rod photoreceptor cells are sensitive to lower-range light intensities and are essential for vision under dim light, whereas cone photoreceptor cells operate at brighter intensities and are essential for daylight, high acuity, and color vision. Retinitis pigmentosa (RP) and age-related macular degeneration (AMD) are retinal degenerative diseases that lead to progressive vision loss because of retinal photoreceptor cell degeneration. RP affects approximately 1.5 million individuals worldwide[1–3] while AMD affects approximately 200 million individuals worldwide.[4] A feature of the retinas of RP and AMD animal models and human patients is outer segment shortening accompanied by photoreceptor dysfunction and degeneration.[5–14] In RP, rod photoreceptor cell degeneration, which initially leads to night blindness, is followed by cone photoreceptor deterioration, eventually resulting in blindness.[15,16] In AMD, deterioration of the macula, the central part of the retina that contains the highest concentration of cone photoreceptor cells, causes loss of central vision.[17] Therefore, understanding the molecular mechanisms that protect cone photoreceptor cells from degeneration under stress conditions, such as in retinal degenerative diseases, is valuable.

The nuclear factor-kappaB (NF-κB) pathway is a signaling cascade that plays key roles in diverse biological processes, including immunity, inflammation, stress responses, and apoptosis. The NF-κB pathway consists of canonical and noncanonical pathways that regulate the subcellular localization and activity of NF-κB, an evolutionarily highly conserved family of transcription factors.[18–23] This pathway is known to be activated in the retina of the RP mouse model and the light-induced retinal degeneration mouse model, which is widely used for studying AMD.[24,25] However, the role and regulatory mechanisms of the NF-κB pathway in retinal photoreceptor cells remain poorly understood.

In the present study, we found that the deubiquitinase Otud7b/Cezanne, whose function in the retina is unknown, is highly expressed in retinal photoreceptor cells. Although *Otud7b*-deficient (*Otud7b*$^{-/-}$) mice exhibited no obvious abnormalities in retinal development and maintenance, cone photoreceptor damage was augmented by *Otud7b* deficiency in mice with light-induced retinal degeneration and RP model mice. RNA-sequencing (RNA-seq) analysis and reporter gene assay showed that the NF-κB pathway is activated in cultured neuronal cells knocked down for *Otud7b* and the retina of *Otud7b*$^{-/-}$ mice. Inhibition of the NF-κB pathway suppressed increased apoptosis in serum-starved cultured neuronal cells and light-induced cone photoreceptor damage in the mouse retina caused by *Otud7b* deficiency. Together,

[1]Laboratory for Molecular and Developmental Biology, Institute for Protein Research, Osaka University, Osaka 565-0871, Japan
[2]Genome Information Research Center, Research Institute for Microbial Diseases, Osaka University, Osaka 565-0871, Japan
[3]Lead contact
*Correspondence: taro.chaya@protein.osaka-u.ac.jp (T.C.), takahisa.furukawa@protein.osaka-u.ac.jp (T.F.)
https://doi.org/10.1016/j.isci.2024.109380

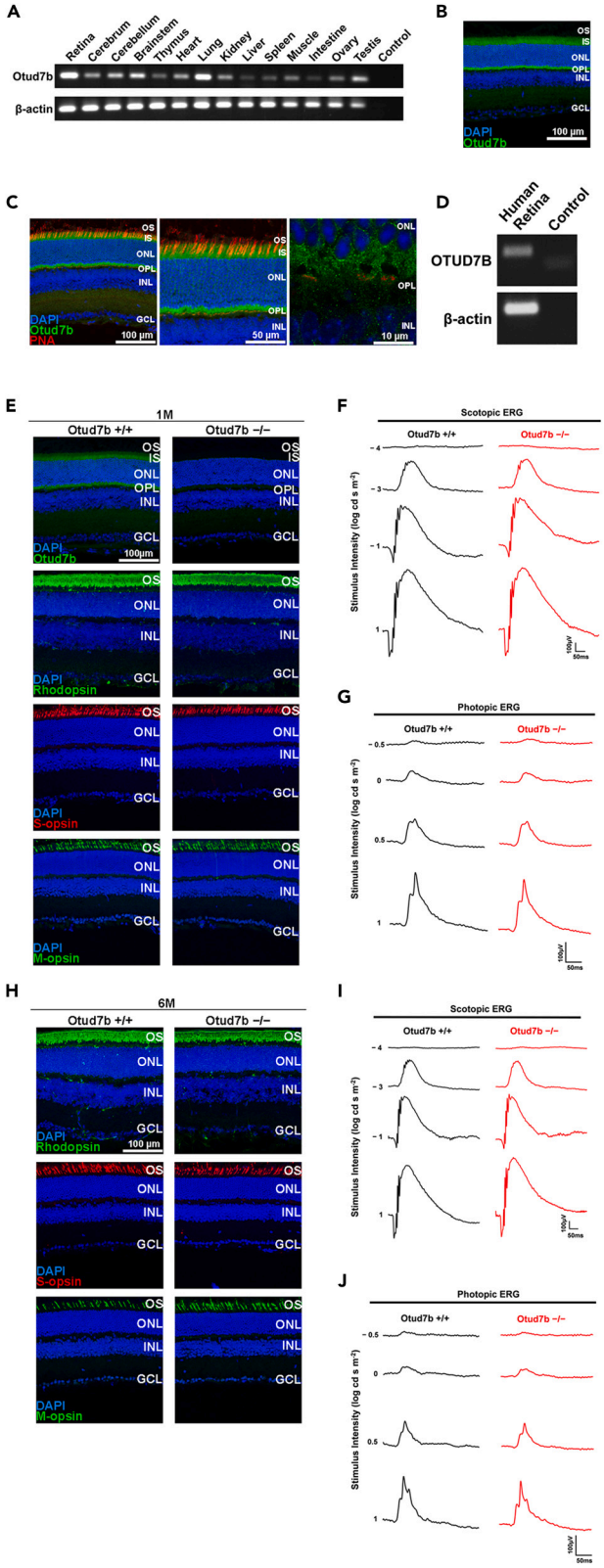
A
Retina
Cerebrum
Cerebellum
Brainstem
Thymus
Heart
Lung
Kidney
Liver
Spleen
Muscle
Intestine
Ovary
Testis
Control
Otud7b
β-actin
B
OS
IS
ONL
OPL
INL
GCL
DAPI
Otud7b
100 μm
C
DAPI
Otud7b
PNA
100 μm
50 μm
10 μm
D
Human Retina
Control
OTUD7B
β-actin
E
1M
Otud7b +/+
Otud7b −/−
DAPI
Otud7b
100μm
Rhodopsin
S-opsin
M-opsin
F
Scotopic ERG
Otud7b +/+
Otud7b −/−
Stimulus Intensity (log cd s m⁻²)
100μV
50ms
G
Photopic ERG
H
6M
I
Scotopic ERG
J
Photopic ERG

Figure 1. Phenotypic analysis of the *Otud7b*$^{-/-}$ mouse retina

(A) RT-PCR analysis of the *Otud7b* transcript in mouse tissues at 4 weeks. *Otud7b* was expressed ubiquitously with strong expression in the retina. *β-actin* was used as a loading control.

(B) Immunofluorescence analysis of the wild-type retina using an anti-Otud7b antibody. Nuclei were stained with DAPI. Otud7b was localized to the photoreceptor inner segment, cell body, and synapse.

(C) Immunofluorescence analysis of the wild-type retina using the anti-Otud7b antibody and PNA (a marker for cone outer segments and synapses). Nuclei were stained with DAPI. Otud7b signals were observed in the vicinity of PNA signals in the OPL.

(D) RT-PCR analysis of the *OTUD7B* transcript in the human retina. *β-actin* was used as a loading control.

(E) Immunofluorescence analysis of retinal sections from *Otud7b*$^{+/+}$ and *Otud7b*$^{-/-}$ mice at 1 M using antibodies against Otud7b, Rhodopsin (a marker for rod outer segments), S-opsin (a marker for S-cone outer segments), and M-opsin (a marker for M-cone outer segments). Nuclei were stained with DAPI. No obvious difference was observed comparing the photoreceptor cells of *Otud7b*$^{+/+}$ and *Otud7b*$^{-/-}$ retinas.

(F and G) ERG analysis of *Otud7b*$^{+/+}$ and *Otud7b*$^{-/-}$ mice at 1 M. (F) Representative scotopic ERGs elicited by four different stimulus intensities (−4.0 to 1.0 log cd s/m^2). (G) Representative photopic ERGs elicited by four stimulus intensities (−0.5 to 1.0 log cd s/m^2).

(H) Immunofluorescence analysis of retinal sections from *Otud7b*$^{+/+}$ and *Otud7b*$^{-/-}$ mice at 6 M using antibodies against Rhodopsin (a marker for rod outer segments), S-opsin (a marker for S-cone outer segments), and M-opsin (a marker for M-cone outer segments). Nuclei were stained with DAPI. No obvious difference was observed between *Otud7b*$^{+/+}$ and *Otud7b*$^{-/-}$ retinas.

(I and J) ERG analysis of *Otud7b*$^{+/+}$ and *Otud7b*$^{-/-}$ mice at 6 M. (I) Representative scotopic ERGs elicited by four stimulus intensities (−4.0 to 1.0 log cd s/m^2). (J) Representative photopic ERGs elicited by four stimulus intensities (−0.5 to 1.0 log cd s/m^2).

OS, outer segment; IS, inner segment; ONL, outer nuclear layer; OPL, outer plexiform layer; INL, inner nuclear layer; GCL, ganglion cell layer.

these results suggest that Otud7b protects cone photoreceptor cells from damage under stress conditions by repressing aberrant activation of the NF-κB pathway.

RESULTS

Otud7b is expressed in retinal photoreceptor cells

We previously reported that the ubiquitin ligase Cul3-Klhl18 regulates transducin translocation during light-dark adaptation in rod photoreceptor cells.[26] To identify other enzymes that are involved in ubiquitin metabolism in the retina and that may regulate photoreceptor function and/or development, we searched for genes enriched in photoreceptor cells. We compared transcripts between control and *Otx2* conditional knockout retinas, in which the cell fate is altered from photoreceptor cells to amacrine-like cells.[27,28] Among the candidate genes identified, we focused on *Otud7b*, the function of which in the retina has not yet been elucidated. To confirm the expression of *Otud7b* in the retina, RT-PCR was performed using various tissues from 4-week-old mice. *Otud7b* was ubiquitously expressed but was highly enriched in the retina (Figure 1A). To investigate the localization of the Otud7b protein in the retina, immunofluorescence analysis was performed on adult mouse retinal sections using an antibody against Otud7b. Otud7b immunofluorescence signals were observed in the inner segment (IS), outer nuclear layer (ONL), and outer plexiform layer (OPL) (Figure 1B). Furthermore, we observed Otud7b signals at the cone photoreceptor synapses marked with peanut agglutinin (PNA) (Figure 1C). In addition, we found the expression of *OTUD7B* in the human retina using RT-PCR (Figure 1D). These results suggest that Otud7b is expressed in rod and cone photoreceptor cells.

Histological and functional analysis of the retina in *Otud7b*$^{-/-}$ mice

To investigate the functional role of Otud7b in retinal photoreceptor cells, we generated conventional *Otud7b*$^{-/-}$ mice using CRISPR/Cas9 genome editing (Figures S1A and S1B). To confirm the loss of Otud7b in the *Otud7b*$^{-/-}$ mouse retina, we performed immunofluorescence analysis and western blotting using an anti-Otud7b antibody. Immunostaining revealed that Otud7b signals were not detected in the *Otud7b*$^{-/-}$ retina, and western blotting revealed that the protein bands observed in the *Otud7b*$^{+/+}$ retina were missing in the *Otud7b*$^{-/-}$ retina, (Figures 1E and S1C). *Otud7b*$^{-/-}$ mice were viable, fertile, and showed no gross morphological abnormalities. To examine the effects of *Otud7b* deficiency on the retina, we performed immunofluorescence analysis on mouse retinal sections at 1 month of age (1 M) using antibodies against Rhodopsin (a marker for rod outer segments), S-opsin (a marker for S-cone outer segments), and M-opsin (a marker for M-cone outer segments); no obvious differences were observed between *Otud7b*$^{+/+}$ and *Otud7b*$^{-/-}$ retinas (Figure 1E). We examined the synapses of photoreceptor cells by immunostaining using antibodies against Pikachurin (a marker for photoreceptor synaptic terminals) and Ctbp2 (a marker for synaptic ribbons); no obvious differences were observed between *Otud7b*$^{+/+}$ and *Otud7b*$^{-/-}$ retinas (Figure S2A). We also examined other cell types using antibodies against Chx10 (a marker for bipolar cells), Pax6 (a marker for amacrine and ganglion cells), Calbindin (a marker for horizontal and a subset of amacrine cells), Rbpms (a marker for ganglion cells), and S100β (a marker for Müller glia) and found no substantial differences between *Otud7b*$^{+/+}$ and *Otud7b*$^{-/-}$ retinas (Figures S2B– S2F). To investigate the physiological effects of *Otud7b* deficiency, we performed electroretinograms (ERGs) under dark (scotopic) and light-adapted (photopic) conditions. The electrical activities of rod photoreceptor cells and rod bipolar cells in response to light stimuli were visualized using the amplitudes of a-waves and b-waves, respectively, under scotopic conditions. In contrast, under photopic conditions, the amplitudes of the a-waves and b-waves reflect the population activity of cone photoreceptors (a-waves) and cone ON-bipolar cells (b-waves). We observed no significant differences in a- and b-wave amplitudes under the scotopic and photopic conditions between *Otud7b*$^{+/+}$ and *Otud7b*$^{-/-}$ mice (Figures 1F, 1G, S3A, and S3B). Next, we examined *Otud7b*$^{+/+}$ and *Otud7b*$^{-/-}$ mouse retinas at 6 months of age (6 M) to investigate whether *Otud7b* deficiency leads to retinal degeneration. Similar to the mouse retinas at 1 M, no substantial differences between *Otud7b*$^{+/+}$ and *Otud7b*$^{-/-}$ mouse retinas

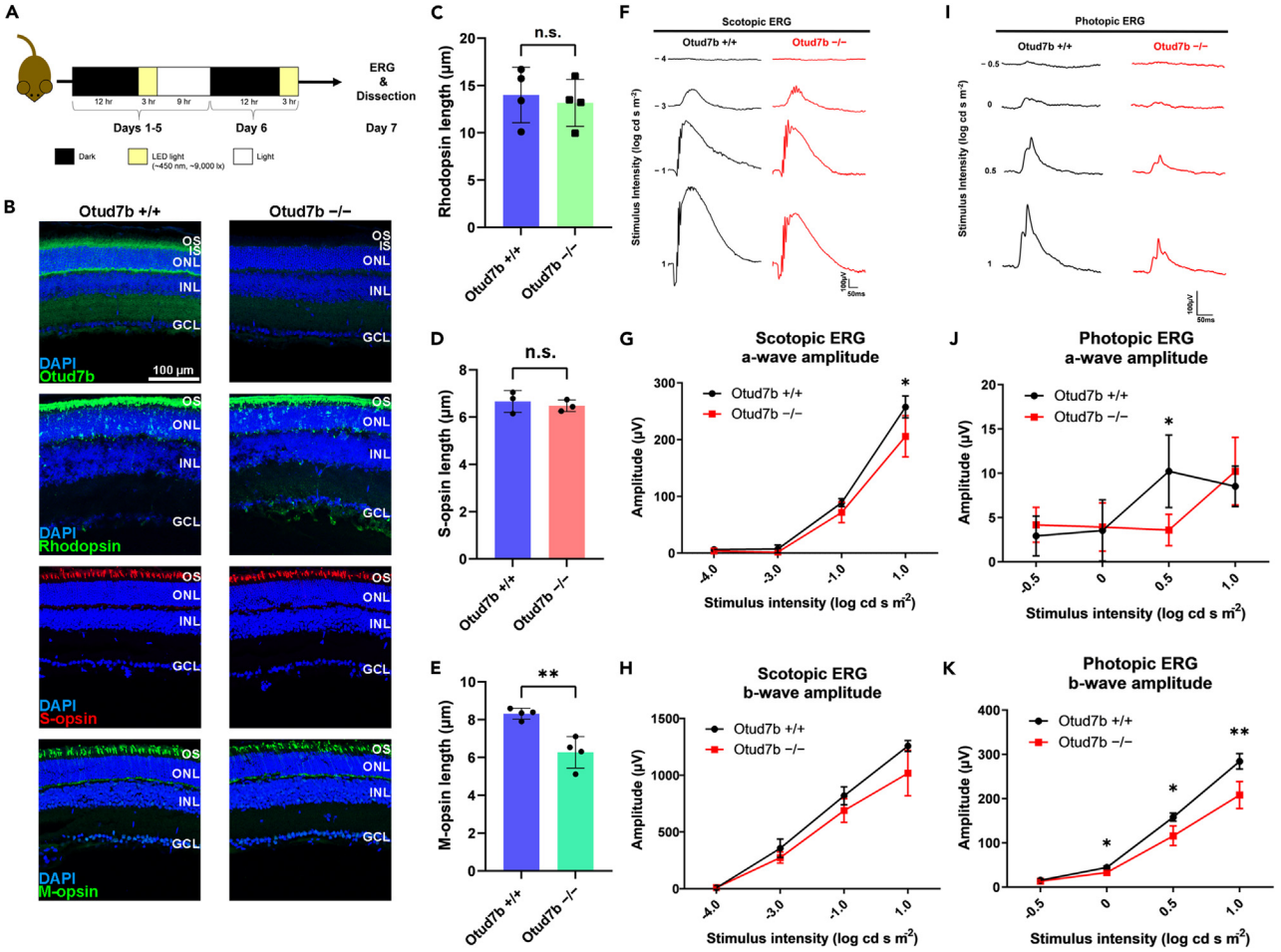

Figure 2. *Otud7b* deficiency exacerbates light-induced retinal damage to cone photoreceptor cells

(A) Schematic representation of the exposure of *Otud7b*$^{+/+}$ and *Otud7b*$^{-/-}$ mice to LED light.

(B) Immunofluorescence analysis of retinal sections from *Otud7b*$^{+/+}$ and *Otud7b*$^{-/-}$ mice after light exposure using antibodies as follows: Otud7b, Rhodopsin (a marker for rod outer segments), S-opsin (a marker for S-cone outer segments), and M-opsin (a marker for M-cone outer segments). Nuclei were stained with DAPI. OS, outer segment; IS, inner segment; ONL, outer nuclear layer; INL, inner nuclear layer; GCL, ganglion cell layer.

(C–E) Rod outer segment (C), S-cone outer segment (D), and M-cone outer segment (E) lengths were measured. M-cone outer segments were shorter in the *Otud7b*$^{-/-}$ retina than in the *Otud7b*$^{+/+}$ retina. **p < 0.01, n.s. not significant (unpaired t-test), n = 4 per genotype.

(F–H) Scotopic ERG analysis of *Otud7b*$^{+/+}$ and *Otud7b*$^{-/-}$ mice after light exposure. (F) Representative scotopic ERGs elicited by four different stimulus intensities (−4.0 to 1.0 log cd s/m^2). Scotopic a-wave (G) and b-wave (H) amplitudes are shown as functions of stimulus intensity. Data are presented as the mean ± SD. *p < 0.05 (unpaired t-test). n = 4 per genotype.

(I–K) Photopic ERG analysis of *Otud7b*$^{+/+}$ and *Otud7b*$^{-/-}$ mice after light exposure. (I) Representative photopic ERGs elicited by four different stimulus intensities (−0.5 to 1.0 log cd s/m^2). Photopic a-wave (J) and b-wave (K) amplitudes are shown as functions of stimulus intensity. Data are presented as the mean ± SD. *p < 0.05, **p < 0.01 (unpaired t-test), n = 4 per genotype.

were observed when immunofluorescence analysis was performed using antibodies against Rhodopsin, S-opsin, and M-opsin (Figure 1H), or when ERGs were recorded (Figures 1I, 1J, S3C, and S3D).

Light-induced retinal damage to cone photoreceptor cells is augmented in *Otud7b*-deficient mice

Next, we investigated the effects of *Otud7b* deficiency on retinas under stress. *Otud7b*$^{-/-}$ mice were exposed to light-emitting diode (LED) light (Figure 2A). Exposure to LED light induces oxidative stress in the retina, which results in photoreceptor degeneration.[29] Immunofluorescence analysis using the anti-Otud7b antibody revealed the absence of Otud7b signal in the light-exposed *Otud7b*$^{-/-}$ retina (Figure 2B). To evaluate histological changes, we performed immunofluorescence analysis using antibodies against Rhodopsin, S-opsin, M-opsin, Iba1, and GFAP to observe the rod outer segments, S-cone outer segments, M-cone outer segments, microglia, and Müller glia, respectively (Figures 2B, S4A, and S4B). No obvious differences were observed in the microglia and Müller glia between light-exposed *Otud7b*$^{+/+}$ and

Otud7b$^{-/-}$ retinas (Figure S4B). There were no significant differences in the lengths of the rod and S-cone outer segments between the light-exposed *Otud7b*$^{+/+}$ and *Otud7b*$^{-/-}$ retinas (Figures 2B–2D). We quantified ONL thickness of light-exposed *Otud7b*$^{+/+}$ and *Otud7b*$^{-/-}$ retinas. There were no significant differences between the *Otud7b*$^{+/+}$ and *Otud7b*$^{-/-}$ retinas (Figure S4C). We also did not observe significant differences in the number of S-cones or M-cones between light-exposed *Otud7b*$^{+/+}$ and *Otud7b*$^{-/-}$ retinas (Figures S4D and S4E). However, M-cone outer segments were significantly shorter in the light-exposed *Otud7b*$^{-/-}$ retinas than in the *Otud7b*$^{+/+}$ retinas, suggesting that M-cone photoreceptor cells were more severely damaged in the light-exposed *Otud7b*$^{-/-}$mice (Figures 2B, 2E, and S4A). Previous studies have reported that outer segment shortening reflects photoreceptor degeneration.[30,31] Additionally, outer segment shortening has been observed in patients with RP.[5,32] Based on these reports, our observations suggest that Otud7b suppresses cone photoreceptor damage under environmental stress. To evaluate physiological changes, we performed ERGs in light-exposed *Otud7b*$^{-/-}$ mice. In the scotopic ERG, the a-wave amplitude at the strongest stimulus showed a significant decrease in *Otud7b*$^{-/-}$ mice (Figures 2F–2H). Under the scotopic conditions, light stimuli below the threshold of −2 log cd s m^{-2} are purely derived from the rod photoreceptor cells; however, stronger light stimuli are derived from both the rod and cone photoreceptor cells.[33] In photopic ERG, *Otud7b*$^{-/-}$ mice had lower photopic amplitudes, which further supports that cone photoreceptor damage increases in light-exposed *Otud7b*$^{-/-}$ mice (Figures 2I–2K). These observations suggest that Otud7b protects cone photoreceptor cells from stress-induced degeneration.

Cone photoreceptor degeneration is intensified by *Otud7b* deficiency in the *Mak*$^{-/-}$ RP model mice

To determine the effects of *Otud7b* deficiency on progressive photoreceptor degeneration, we mated *Otud7b*$^{-/-}$ mice with male germ cell-associated kinase knockout (*Mak*$^{-/-}$) mice. We previously reported that *Mak* is highly expressed in retinal photoreceptor cells and that *Mak*$^{-/-}$ mice exhibit progressive photoreceptor degeneration.[34,35] Subsequent analyses have shown that mutations in the human *MAK* gene are associated with RP.[36,37] Immunofluorescence analysis was performed using antibodies against Rhodopsin, S-opsin, M-opsin, and Gnat2 (a marker for cone outer segments) in *Otud7b*$^{-/-}$; *Mak*$^{-/-}$ retinas (Figure 3A). Although there were no obvious differences in rod outer segments between the *Otud7b*$^{+/+}$; *Mak*$^{-/-}$ and *Otud7b*$^{-/-}$; *Mak*$^{-/-}$ retinas, the *Otud7b*$^{-/-}$; *Mak*$^{-/-}$ retinas had shorter cone outer segments than the *Otud7b*$^{+/+}$; *Mak*$^{-/-}$ retinas (Figure 3B). In addition, we observed that ONL thickness decreased in the *Otud7b*$^{-/-}$; *Mak*$^{-/-}$ retina (Figure 3C). In contrast, the thickness of the other retinal layers did not differ significantly between *Otud7b*$^{+/+}$; *Mak*$^{-/-}$ and *Otud7b*$^{-/-}$; *Mak*$^{-/-}$ mice (Figure 3D). Next, we examined the electrophysiological properties of *Otud7b*$^{-/-}$; *Mak*$^{-/-}$ mice by ERG analysis. While we did not observe a significant difference in the scotopic ERGs (Figures 3E–3G), the photopic ERG b-wave amplitudes were significantly lower in *Otud7b*$^{-/-}$; *Mak*$^{-/-}$ mice than in *Otud7b*$^{+/+}$; *Mak*$^{-/-}$ mice (Figures 3H–3J). Consistent with the results obtained from the light exposure experiments (Figure 2), these results suggest that Otud7b suppresses cone photoreceptor degeneration under stress conditions.

Otud7b-deficient neuronal cells are susceptible to cell death under stress

We investigated the role of Otud7b in neuronal cells cultured under stress from serum starvation, an environmental stress that has been shown to induce oxidative stress.[38,39] We constructed plasmids expressing a short hairpin RNA (shRNA) to knockdown *Otud7b* and confirmed by western blotting that Otud7b-shRNA1 was able to suppress Otud7b expression (Figure 4A). Plasmids encoding shRNA-control or Otud7b-shRNA1 were transfected into the murine neuronal cell line, Neuro2A. These cells were starved of serum for 14 h before immunofluorescence analysis using an antibody against cleaved caspase 3 (a marker of apoptosis) or Otud7b (Figures 4B and S5A). We observed that Otud7b signals markedly decreased in the cells expressing Otud7b-shRNA1 but not in those expressing shRNA-control, indicating that *Otud7b* was knocked down in Neuro2A cells by Otud7b-shRNA1 (Figure S5A). We quantified cleaved caspase 3 and GFP double-positive cells and normalized them to GFP-positive cells. Neuro2A cells transfected with Otud7b-shRNA1 had more double-positive cells than those transfected with shRNA-control (Figure 4C). In addition, a cell viability assay was performed to compare the Neuro2A cells expressing shRNA-control with those expressing Otud7b-shRNA1 (Figures S5B and S5C). Neuro2A cells expressing the Otud7b-shRNA1 showed a decrease in cell viability compared to those expressing the shRNA-control (Figure S5C). However, no significant difference in the number of double-positive cells was observed between the shRNA-control and Otud7b-shRNA1-expressing cells without serum starvation (Figures S5D and S5E). To confirm these results, we used small interfering RNAs (siRNAs) to knock down *Otud7b* in Neuro2A cells. After confirming the knockdown efficiency of the siRNAs (Figure 4D), we transfected Otud7b-siRNAs into Neuro2A cells that were then cultured in serum-free medium. We performed immunofluorescence analysis using an anti-Otud7b antibody and observed that Otud7b-positive cells markedly decreased in the cells transfected with Otud7b-siRNA3 or Otud7b-siRNA4 compared with the cells transfected with the siRNA-control (Figure S5F). Immunofluorescence analysis of serum-starved cells revealed an increase in cleaved caspase 3-positive cells among cells transfected with Otud7b-siRNAs (Figures 4E and 4F). We performed western blot analysis and observed an increase in cleaved caspase 3 in Neuro2A cells transfected with Otud7b-siRNA3 or Otud7b-siRNA4 after serum starvation (Figure S5G). Furthermore, a significant reduction in cell viability was observed in the serum-starved cells transfected with the Otud7b-siRNA4, while the serum-starved cells transfected with the Otud7b-siRNA3 showed a tendency to decrease cell viability (Figures S5H and S5I). Additionally, we treated Neuro2A cells with 10 μM H_2O_2 for 20 h to induce oxidative stress and performed immunofluorescence analysis using an anti-cleaved caspase 3 antibody (Figures S5J and S5K). The percentage of cleaved caspase 3-positive cells significantly increased in the H_2O_2-treated cells transfected with Otud7b-siRNA3 and Otud7b-siRNA4 compared to those transfected with the siRNA-control (Figures S5J and S5K). These results suggest that Otud7b protects neuronal cells from stress-induced damage.

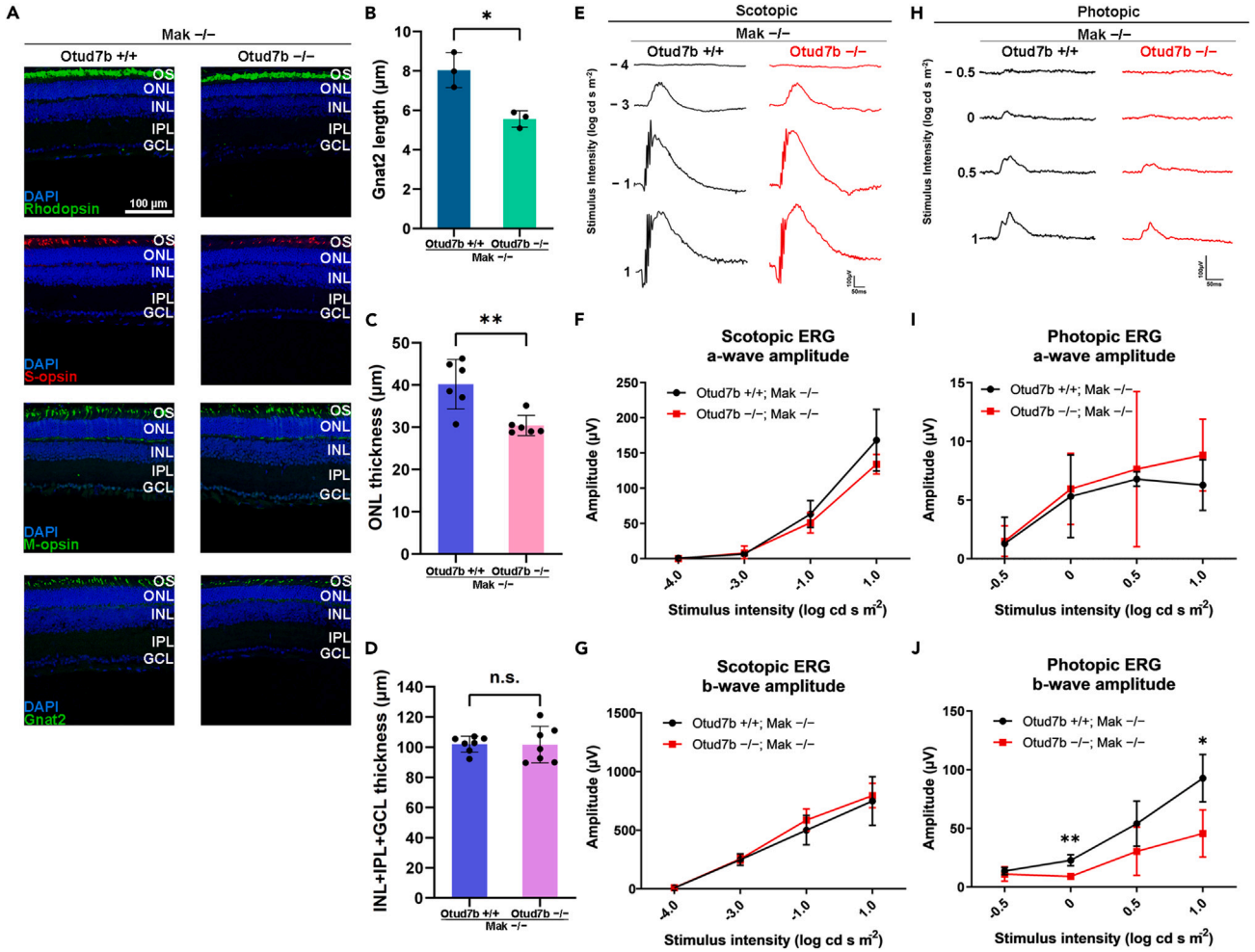

Figure 3. *Otud7b* deficiency exacerbates retinal degeneration in *Mak*$^{-/-}$ mice

(A) Immunofluorescence analysis of retinal sections from *Otud7b*$^{+/+}$; *Mak*$^{-/-}$ and *Otud7b*$^{-/-}$; *Mak*$^{-/-}$ at 2 M using antibodies against Rhodopsin (a marker for rod outer segments), S-opsin (a marker for S-cone outer segments), M-opsin (a marker for M-cone outer segments), and Gnat2 (a marker for cone outer segments). Nuclei were stained with DAPI. OS, outer segment; ONL, outer nuclear layer; INL, inner nuclear layer; IPL, inner plexiform layer; GCL, ganglion cell layer.

(B) Cone outer segment length was measured in *Otud7b*$^{+/+}$; *Mak*$^{-/-}$ and *Otud7b*$^{-/-}$; *Mak*$^{-/-}$ retinas at 2 M *Otud7b*$^{-/-}$; *Mak*$^{-/-}$ retinas had significantly shorter cone outer segments. Data are presented as the mean ± SD. *p < 0.05 (unpaired t-test), n = 3 per genotype.

(C) The ONL thickness was measured. The ONL thickness in the *Otud7b*$^{-/-}$; *Mak*$^{-/-}$ retina was significantly thinner than that in the *Otud7b*$^{+/+}$; *Mak*$^{-/-}$ retina. Data are presented as the mean ± SD. **p < 0.01 (unpaired t-test), n = 6 retinal sections from 3 mice per genotype.

(D) The INL+IPL+GCL thickness was measured. Data are presented as the mean ± SD. n.s., not significant (unpaired t-test). n = 6 retinal sections from 3 mice per genotype.

(E–G) Scotopic ERG analysis of *Otud7b*$^{+/+}$; *Mak*$^{-/-}$ and *Otud7b*$^{-/-}$; *Mak*$^{-/-}$ mice at 2 M. (E) Representative scotopic ERGs elicited by four different stimulus intensities (−4.0 to 1.0 log cd s/m^2). Scotopic a-wave (F) and b-wave (G) amplitudes are shown as functions of stimulus intensity. Data are presented as the mean ± SD (unpaired t-test). n = 3 per genotype.

(H–J) Photopic ERG analysis of *Otud7b*$^{+/+}$; *Mak*$^{-/-}$ and *Otud7b*$^{-/-}$; *Mak*$^{-/-}$ mice at 2 M. (H) Representative photopic ERGs elicited by four stimulus intensities (−0.5 to 1.0 log cd s/m^2). Photopic a-wave (I) and b-wave (J) amplitudes are shown as functions of stimulus intensity. Data are presented as the mean ± SD. *p < 0.05, **p < 0.01 (unpaired t-test). n = 3 per genotype.

NF-κB is activated by *Otud7b* deficiency

To gain insights into how neuronal cell damage is enhanced by *Otud7b* deficiency in cultured cells and *in vivo*, we performed RNA-seq analysis using retinal RNAs from *Otud7b*$^{+/+}$ and *Otud7b*$^{-/-}$ mice exposed to light. Ingenuity pathway analysis (IPA) revealed that the genes encoding transcription regulators of Cebpa, Rela, Ebf1, Cebpd, Spi1, Ncoa1, Id3, and Srebf1 were upregulated in light-exposed *Otud7b*$^{-/-}$ retina (Z scores >2) (Figure 5A). The IPA networks showed that the transcription factor RelA was an upstream regulator (Figure 5B). RelA is one of the five NF-κB proteins known to form dimers with four other proteins that regulate NF-κB activity.[40,41] Activation of NF-κB has been

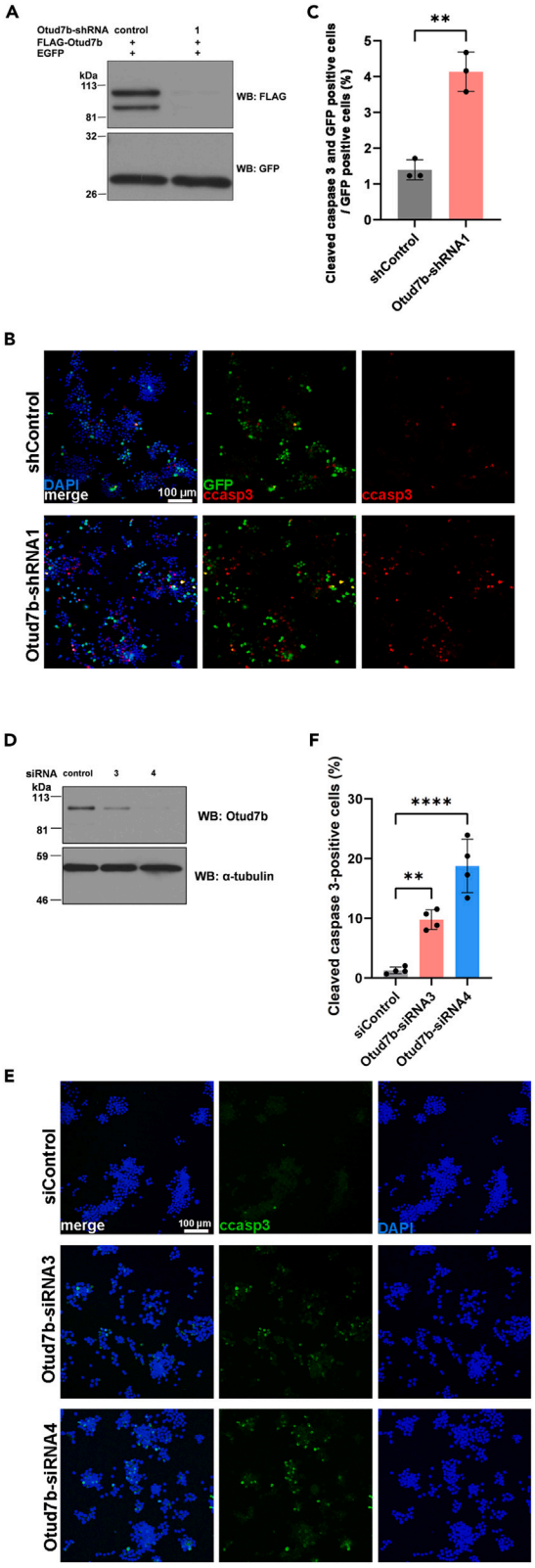
A
Otud7b-shRNA control 1
FLAG-Otud7b + +
EGFP + +
kDa
113
81
32
26
WB: FLAG
WB: GFP
C
Cleaved caspase 3 and GFP positive cells / GFP positive cells (%)
**
shControl
Otud7b-shRNA1
B
shControl
Otud7b-shRNA1
DAPI
merge
100 μm
GFP
ccasp3
ccasp3
D
siRNA control 3 4
kDa
113
81
59
46
WB: Otud7b
WB: α-tubulin
F
Cleaved caspase 3-positive cells (%)
****
**
siControl
Otud7b-siRNA3
Otud7b-siRNA4
E
siControl
Otud7b-siRNA3
Otud7b-siRNA4
merge
100 μm
ccasp3
DAPI

Figure 4. Knockdown of *Otud7b* in neuronal cells increases susceptibility to cell death under stress

(A) Inhibition efficacy of shRNA expression constructs for *Otud7b* knockdown. ShRNA-control or Otud7b-shRNA1 expression plasmids were co-transfected with plasmids expressing an FLAG-tagged Otud7b and a GFP into HEK293T cells. Western blotting was performed using anti-FLAG and anti-GFP antibodies. GFP was used as an internal transfection control. Otud7b-shRNA1 effectively suppressed Otud7b expression.

(B and C) ShRNA-control or Otud7b-shRNA1 expression plasmids were co-transfected with a plasmid expressing EGFP into Neuro2A cells. The cells were serum starved for 14 h. (B) Immunofluorescence analysis was performed using an anti-cleaved caspase 3 antibody. Nuclei were stained with DAPI. Increased number of cleaved caspase 3 and GFP double-positive cells was observed in the Otud7b-shRNA1 transfected cells. (C) The number of cleaved caspase 3 and GFP double-positive cells per GFP-positive cells was measured. Data are presented as the mean ± SD. **p < 0.01 (unpaired t-test). n = 3 experiments.

(D) Inhibition efficacy of siRNAs for *Otud7b* knockdown. SiRNA-control, Otud7b-siRNA3, or Otud7b-siRNA4 was transfected into Neuro2A cells. Western blotting was performed using antibodies against Otud7b and α-tubulin. α-tubulin was used as a loading control. Otud7b-siRNA3 and Otud7b-siRNA4 effectively suppressed Otud7b expression.

(E and F) Neuro2A cells were transfected with siRNA-control, Otud7b-siRNA3, or Otud7b-siRNA4. The cells were serum starved for 14 h. (E) Immunofluorescence analysis was performed with an anti-cleaved caspase 3 antibody. Nuclei were stained with DAPI. Increased number of cleaved caspase 3-positive cells was observed in the cells transfected with Otud7b-siRNA3 and Otud7b-siRNA4. (F) The number of cleaved caspase 3-positive cells was measured. Data are presented as the mean ± SD. **p < 0.01, ****p < 0.0001 (one-way ANOVA followed by Tukey's multiple comparisons test). n = 4 experiments.

associated with retinal degeneration.[24] We performed immunofluorescence analysis of RelA in light-exposed *Otud7b*$^{+/+}$ and *Otud7b*$^{-/-}$ retinas (Figure 5C). We detected a significant increase in RelA signals in the ONL of light-exposed *Otud7b*$^{-/-}$ retinas, suggesting that NF-κB is activated in photoreceptor cells of the light-exposed *Otud7b*$^{-/-}$ retina compared to that in the light-exposed *Otud7b*$^{+/+}$ retina (Figure 5D). We next analyzed NF-κB activation in the serum-starved Neuro2A cell lysates using a NanoLuc luciferase reporter construct driven by an NF-κB response element and minimal promoter and observed that luciferase activity increased in the *Otud7b* knockdown cells (Figures 5E and 5F). These results suggest that Otud7b suppresses aberrant NF-κB activation.

Neuronal cell death resulting from *Otud7b* knockdown is suppressed by NF-κB pathway inhibition

Based on the results of the IPA analysis and NanoLuc-luciferase (Figure 5), we hypothesized NF-κB as a factor for Neuro2A cell death and photoreceptor degeneration caused by *Otud7b* deficiency. To test this hypothesis, we examined the effects of curcumin, an inhibitor of the NF-κB pathway, on neuronal cell death induced by *Otud7b* knockdown under stress conditions. Neuro2A cells expressing Otud7b-siRNAs were treated with curcumin, and immunofluorescence analysis was performed to observe apoptotic cells (Figures 6A and 6B). We observed no significant difference in the number of cleaved caspase 3-positive cells between cells expressing siRNA-control treated with DMSO and those treated with curcumin; however, the increase in cleaved caspase 3-positive cells induced by Otud7b-siRNAs was suppressed by curcumin treatment (Figures 6A and 6B). In addition, immunofluorescence analysis of RelA revealed that curcumin repressed the increased nuclear localization of RelA in the cells transfected with Otud7b-siRNAs (Figure 6C). In addition, immunofluorescence analysis of RelA revealed that curcumin repressed the increased nuclear-to-cytoplasmic ratio of RelA in the cells transfected with Otud7b-siRNAs (Figures 6C and S5L). To confirm these results, we performed similar experiments using another NF-κB inhibitor, BMS-345541 (Figures 6D and 6E). *Otud7b* knockdown cells treated with BMS-345541 also showed significantly decreased numbers of cleaved caspase 3-positive cells compared to those treated with DMSO (Figures 6D and 6E). Similar to the results for curcumin, BMS-345541 also repressed the increased nuclear localization of RelA in the cells transfected with Otud7b-siRNAs (Figure 6F). These results suggest that Otud7b protects neuronal cells from cell damage by downregulating NF-κB activation under stress conditions.

Light-induced retinal damage augmented by *Otud7b* deficiency is repressed by NF-κB pathway inhibition

We stained both retinal flat mounts and sections using PNA, assessed the number of cones, and found that there were no significant differences between the light-exposed *Otud7b*$^{+/+}$ and *Otud7b*$^{-/-}$ retinas treated with DMSO (Figures S6A–S6D). We then examined the cone outer segment length from the retinal sections and found that the cone outer segment lengths of *Otud7b*$^{-/-}$ retinas were significantly shorter than those of *Otud7b*$^{+/+}$ retinas (Figures S6C and S6E). To examine whether the inhibition of NF-κB would rescue the phenotypes observed in *Otud7b*$^{-/-}$ mouse retinas under stress conditions, we exposed *Otud7b*$^{-/-}$ mice injected with curcumin to LED light (Figure 7A). We analyzed the histological changes by immunofluorescence using antibodies against Rhodopsin, S-opsin-, and M-opsin (Figures 7B–7D). No significant differences were observed in the outer segments of the rod and S-cones between *Otud7b*$^{+/+}$ and *Otud7b*$^{-/-}$ mice treated with or without curcumin (Figures 7B, 7C, 7E, and 7F). The numbers of S-cones and M-cones also did not show a significant difference (Figures S6F and S6G). However, the decrease in the M-cone outer segment length in the *Otud7b*$^{-/-}$ retina was suppressed by curcumin (Figures 7D and 7G). We observed a significant increase in cells that express cleaved caspase 3 in the ONL of the retina from *Otud7b*$^{-/-}$ mice treated with DMSO compared to those from *Otud7b*$^{+/+}$ mice treated with DMSO, whereas curcumin treatment reduced the number of cleaved caspase 3 in the ONL of *Otud7b*$^{-/-}$ retinas (Figures 7H and 7I). These results suggest that Otud7b suppresses light-induced retinal damage by downregulating NF-κB activation. In addition, we performed immunofluorescence analysis using an anti-RelA antibody and measured the RelA signal intensity in the ONL of light-exposed DMSO-treated and curcumin-treated *Otud7b*$^{-/-}$ retinas (Figures 7J and 7K). The RelA signal intensity in the ONL decreased significantly in the curcumin-treated *Otud7b*$^{-/-}$ mice compared to that in the DMSO-treated *Otud7b*$^{-/-}$ mice, suggesting that the increased NF-κB activity in photoreceptor cells of the *Otud7b*$^{-/-}$ retina is suppressed by curcumin (Figure 7K). To confirm these results, we exposed *Otud7b*$^{+/+}$ and *Otud7b*$^{-/-}$ mice injected with BMS-345541 to LED light (Figure 8A). Immunofluorescence analysis using antibodies against Rhodopsin, S-opsin, and M-opsin were used to observe the histological changes (Figures 8B–8D). Similar to the

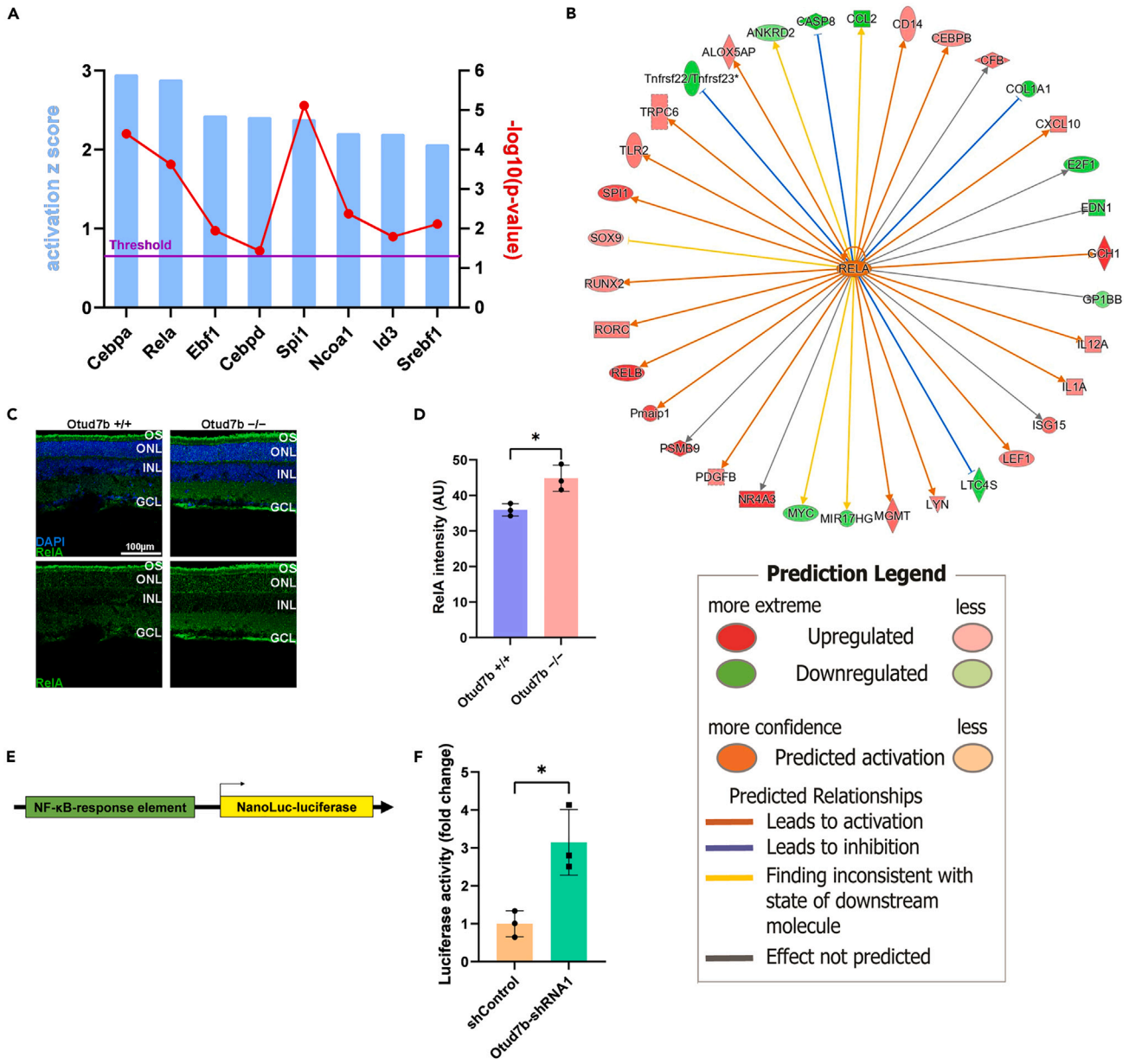

Figure 5. NF-κB is activated by *Otud7b* deficiency

(A) IPA to predict the upstream transcription regulators affecting gene expression changes (fold change >1.5 or < −1.5; FPKM >0.2) in the *Otud7b*$^{-/-}$ retina after light exposure. The transcription regulators with activation Z scores >2 and $p < 0.05$ are shown.

(B) The IPA networks showing the transcription factor RelA as an upstream regulator. RelA is predicted to be activated in *Otud7b*$^{-/-}$ retina after light exposure. IPA, ingenuity pathway analysis.

(C) Immunofluorescence analysis of retinal sections from *Otud7b*$^{+/+}$ and *Otud7b*$^{-/-}$ mice after light exposure using an anti-RelA antibody. Nuclei were stained with DAPI. OS, outer segment; ONL, outer nuclear layer; INL, inner nuclear layer; GCL, ganglion cell layer.

(D) RelA signal intensity in the ONL of *Otud7b*$^{+/+}$ and *Otud7b*$^{-/-}$ retinas after light exposure was measured. RelA signal intensity in the ONL increased in the *Otud7b*$^{-/-}$ retina. Data are presented as the mean ± SD. *$p < 0.05$ (unpaired t-test). n = 3 experiments.

(E) Schematic diagram of the NF-κB response element and minimal promoter.

(F) ShRNA-control or Otud7b-shRNA1 expression plasmids were co-transfected into Neuro2A cells with a *NanoLuc luciferase* reporter construct driven by an NF-κB response element and minimal promoter as well as a *Firefly luciferase*-expressing construct driven by a minimal promoter. Luciferase activity of the cell lysates was measured 14 h after serum starvation. NanoLuc luciferase activity was normalized to Firefly luciferase activity. Data are presented as the mean ± SD. *$p < 0.05$ (unpaired t-test). n = 3 experiments.

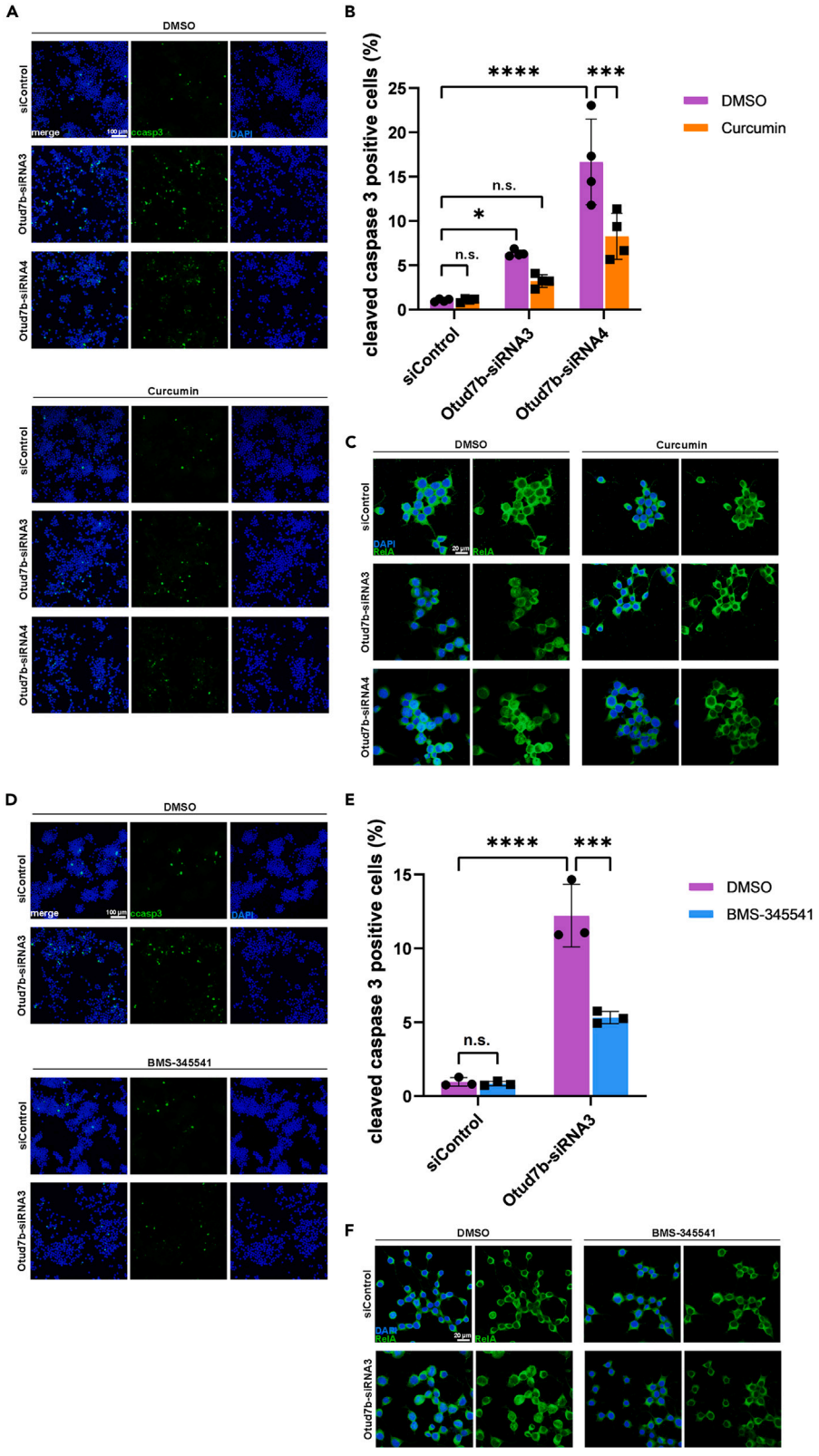
A
DMSO
siControl
Otud7b-siRNA3
Otud7b-siRNA4
merge
casp3
DAPI
Curcumin
B
cleaved caspase 3 positive cells (%)
****
***
n.s.
*
n.s.
DMSO
Curcumin
siControl
Otud7b-siRNA3
Otud7b-siRNA4
C
DMSO
Curcumin
DAPI
RelA
D
DMSO
BMS-345541
E
cleaved caspase 3 positive cells (%)
DMSO
BMS-345541
F
DMSO
BMS-345541

Figure 6. NF-κB pathway inhibition reduces cell death induced by *Otud7b* knockdown

(A) Neuro2A cells treated with curcumin were transfected with siRNA-control, Otud7b-siRNA3, or Otud7b-siRNA4. The cells were serum starved for 24 h in a medium containing curcumin. Cells were immunostained with an anti-cleaved caspase 3 antibody. Nuclei were stained with DAPI.

(B) The number of cleaved caspase 3-positive cells was counted. Curcumin treatment suppressed the increase of cleaved caspase 3-positive cells caused by *Otud7b* knockdown. Data are presented as the mean ± SD. *p < 0.05, ***p < 0.001 ****p < 0.0001, n.s. not significant (two-way ANOVA followed by Tukey's multiple comparisons test). n = 4 experiments.

(C) Immunofluorescence analysis of serum starved Neuro2A cells using an anti-RelA antibody. Curcumin suppressed the nuclear localization of RelA. Nuclei were stained with DAPI.

(D) Neuro2A cells treated with BMS-345541 were transfected with siRNA-control or Otud7b-siRNA3. The cells were serum starved for 24 h in the medium containing BMS-345541. Cells were immunostained with an anti-cleaved caspase 3 antibody. Nuclei were stained with DAPI.

(E) The number of cleaved caspase 3-positive cells was counted. BMS-345541 treatment suppressed the increase of cleaved caspase 3-positive cells caused by *Otud7b* knockdown. Data are presented as the mean ± SD. ***p < 0.001 ****p < 0.0001, n.s. not significant (two-way ANOVA followed by Tukey's multiple comparisons test). n = 3 experiments.

(F) Immunofluorescence analysis of serum starved Neuro2A cells using an anti-RelA antibody. BMS-345541 suppressed the nuclear localization of RelA. Nuclei were stained with DAPI.

curcumin-treated mice, rod and S-cone outer segment lengths did not show a significant difference (Figures 8E and 8F). In contrast, the decrease in the M-cone outer segment lengths of the *Otud7b*$^{-/-}$ retina was suppressed by BMS-345541 (Figure 8G). There was no significant difference in the number of S-cones or M-cones between *Otud7b*$^{+/+}$ and *Otud7b*$^{-/-}$ mice treated with either DMSO or BMS-345541 (Figures S7A and S7B). In addition, the increased number of cleaved caspase 3-positive cells in the ONL of the light-exposed *Otud7b*$^{-/-}$ retina was reduced by BMS-345541 treatment (Figures 8H and 8I). Furthermore, we performed immunofluorescence analysis of RelA and measured RelA signal intensity in the ONL of the retina from light-exposed *Otud7b*$^{-/-}$ mice treated with either DMSO or BMS-345541 (Figures 8J and 8K). The RelA signal intensity in the ONL decreased significantly in BMS-345541-treated *Otud7b*$^{-/-}$ mice compared to that in DMSO-treated *Otud7b*$^{-/-}$ mice (Figure 8K). These results further support the idea that Otud7b suppresses light-induced retinal damage by downregulating NF-κB activation.

DISCUSSION

In this study, we found that Otud7b was highly expressed in retinal photoreceptor cells. We did not observe that ablation of *Otud7b* affects retinal photoreceptor development and function; however, cone photoreceptor damage was enhanced in the retinas of *Otud7b*$^{-/-}$ mice subjected to stress conditions by exposure to intense light or mating with the *Mak*$^{-/-}$ RP model mice. We also found that *Otud7b* knockdown in cultured neuronal cells subjected to serum starvation increased cell death. RNA-seq analysis and reporter gene assay showed that NF-κB is activated by *Otud7b* deficiency. Inhibition of the NF-κB pathway ameliorated cone degeneration and neuronal cell death caused by the loss of *Otud7b* in the retina and *Otud7b* knockdown in cultured cells, respectively. These findings suggest that Otud7b protects cone photoreceptor cells from degeneration through the inhibition of the NF-κB in the retina.

The M-cone outer segments, but not the S-cone outer segments, were shorter in light-exposed *Otud7b*$^{-/-}$ mouse retinas than in light-exposed *Otud7b*$^{+/+}$ mouse retinas. M-cone and S-cone photoreceptor cells are mainly located on the dorsal/superior and ventral/inferior sides of the retina, respectively.[42] Given that light-induced damage, an AMD model,[24,25] has been reported to significantly impact the dorsal/superior side of the retina compared to the ventral/inferior side,[29,43] phenotypic differences between M-cone and S-cone outer segment lengths in the light-exposed *Otud7b*$^{-/-}$ retina might be due to the locations of M-cone and S-cone photoreceptor cells in the retina. In addition, photopic ERG amplitudes indicated greater impairment in cone photoreceptor function in light-exposed *Otud7b*$^{-/-}$ mice than in light-exposed *Otud7b*$^{+/+}$ mice. In contrast to cone photoreceptor cells, the outer segments of rod photoreceptors in *Otud7b*$^{+/+}$ and *Otud7b*$^{-/-}$ mouse retinas exposed to intense light did not exhibit a significant difference. Furthermore, scotopic ERG amplitudes were almost unchanged in *Otud7b*$^{+/+}$ and *Otud7b*$^{-/-}$ mice subjected to light-damage experiments. Taken together, these results suggest that Otud7b functions more in cone photoreceptor cells than in rod photoreceptor cells under intense light.

We also investigated the effects of *Otud7b* ablation in an RP model *Mak*$^{-/-}$ mice. In this model, progressive retinal deterioration of rods and cones begins at approximately 1 M.[34] A significant decrease in ONL thickness was observed in the *Otud7b*$^{-/-}$; *Mak*$^{-/-}$ mouse retina compared to that in the *Otud7b*$^{+/+}$; *Mak*$^{-/-}$ mouse retina; however, scotopic ERG did not indicate a significant difference between the *Otud7b*$^{+/+}$; *Mak*$^{-/-}$ and *Otud7b*$^{-/-}$; *Mak*$^{-/-}$ mouse retinas, suggesting that rod photoreceptor cell function is not drastically altered by *Otud7b* deficiency. Notably, the outer segments of cone photoreceptor cells were significantly shorter in *Otud7b*$^{-/-}$; *Mak*$^{-/-}$ retinas than in *Otud7b*$^{+/+}$; *Mak*$^{-/-}$ retinas. In addition, photopic ERG indicated decreased cone photoreceptor function in *Otud7b*$^{-/-}$; *Mak*$^{-/-}$ retinas. These results imply that Otud7b mitigates cone photoreceptor degeneration under stress conditions. Given that *OTUD7B* was also found to be expressed in the human retina, mutations and/or variants of the *OTUD7B* gene may be disease modifiers of AMD and RP.

The cleaved caspase 3-positive cells significantly increased in the ONL of the light-exposed *Otud7b*$^{-/-}$ mice compared with that of the light-exposed *Otud7b*$^{+/+}$ mice. However, we observed no significant change in the number of cone photoreceptor cells between the light-exposed *Otud7b*$^{+/+}$ and *Otud7b*$^{-/-}$ mice. One possible explanation of this result may be that more time is needed after light exposure to observe significant cone photoreceptor cell loss. Another possible explanation may be that the percentage of cone photoreceptor cells that expressed cleaved caspase 3 is too low to impact the cell number.

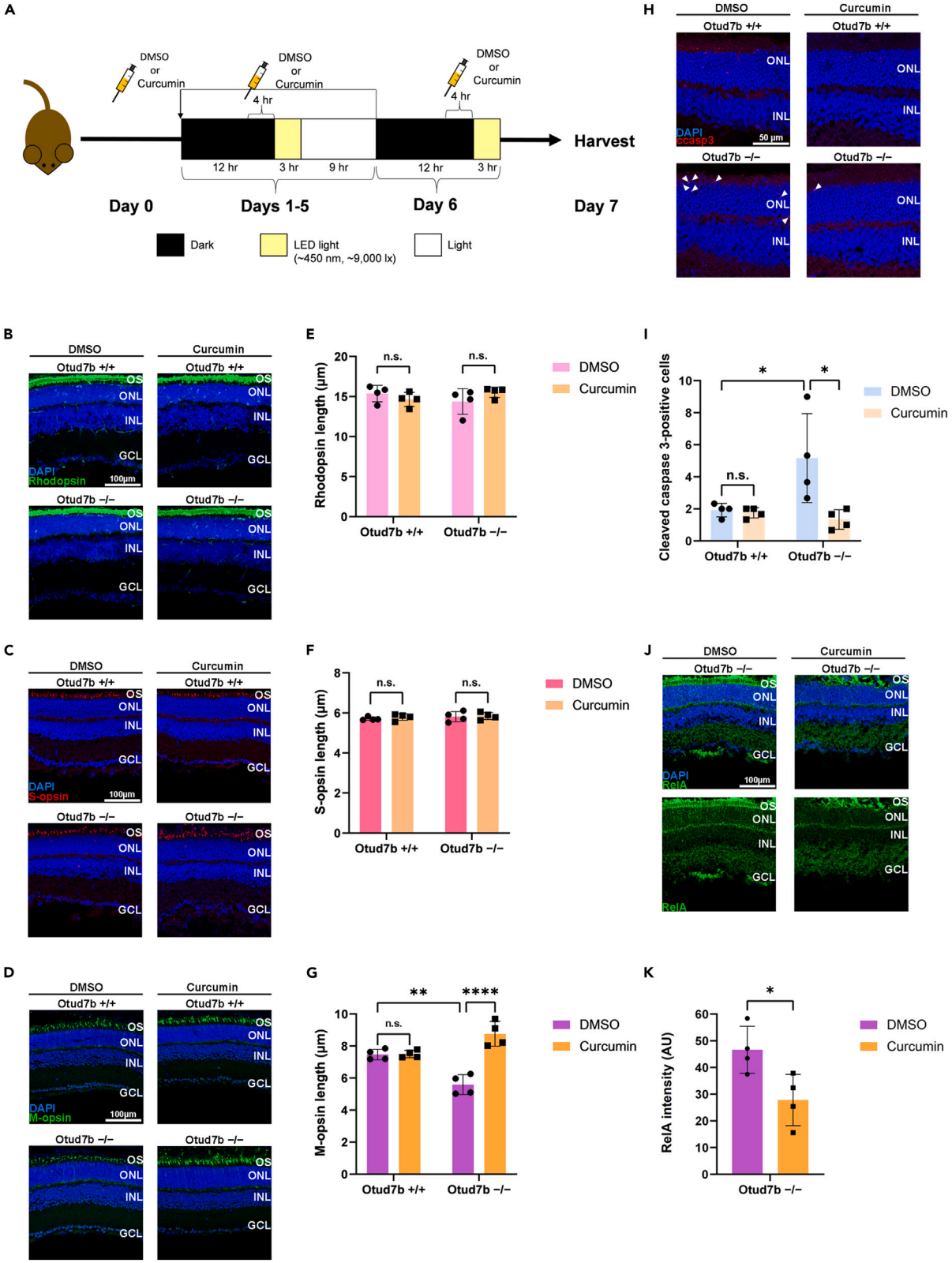
A
DMSO or Curcumin
DMSO or Curcumin
4 hr
DMSO or Curcumin
4 hr
12 hr
3 hr
9 hr
12 hr
3 hr
Harvest
Day 0
Days 1-5
Day 6
Day 7
Dark
LED light (~450 nm, ~9,000 lx)
Light
H
DMSO
Curcumin
Otud7b +/+
Otud7b −/−
ONL
INL
DAPI
ccasp3
50 μm
B
DMSO
Curcumin
Otud7b +/+
Otud7b −/−
OS
ONL
INL
GCL
DAPI
Rhodopsin
100μm
E
Rhodopsin length (μm)
n.s.
DMSO
Curcumin
I
Cleaved caspase 3-positive cells
*
n.s.
C
S-opsin
F
S-opsin length (μm)
J
RelA
D
M-opsin
G
M-opsin length (μm)
**
****
K
RelA intensity (AU)

Figure 7. NF-κB pathway inhibition suppresses light-induced retinal damage in *Otud7b*$^{-/-}$ mice

(A) Schematic representation of LED light exposure to mice treated with curcumin. Curcumin was injected into mice every day for 7 days.

(B–D) Immunofluorescence analysis of retinal sections from curcumin-treated *Otud7b*$^{+/+}$ and *Otud7b*$^{-/-}$ mice after light exposure using the following antibodies: Rhodopsin (a marker for rod outer segments, B), S-opsin (a marker for S-cone outer segments, C), and M-opsin (a marker for M-cone outer segments, D). Nuclei were stained with DAPI.

(E–G) Rod outer segment (E), S-cone outer segment (F), and M-cone outer segment (G) lengths measured in curcumin-treated *Otud7b*$^{+/+}$ and *Otud7b*$^{-/-}$ mice after light exposure. The M-cone outer segments were longer in curcumin-treated *Otud7b*$^{-/-}$ retina compared to DMSO-treated *Otud7b*$^{-/-}$ retina. **p < 0.01, ****p < 0.0001, n.s. not significant (two-way ANOVA followed by Tukey's multiple comparisons test), n = 4 per genotype.

(H) Immunofluorescence analysis of retinal sections from curcumin-treated *Otud7b*$^{+/+}$ and *Otud7b*$^{-/-}$ mice after light exposure using an anti-cleaved caspase 3 antibody. Nuclei were stained with DAPI. White arrows indicate cleaved caspase 3-positive cells.

(I) The number of cleaved caspase 3-positive cells was counted. Curcumin treatment significantly reduced the number of cleaved caspase 3-positive cells in the *Otud7b*$^{-/-}$ retina. *p < 0.05, n.s. not significant (two-way ANOVA followed by Tukey's multiple comparisons test), n = 4 per genotype.

(J) Immunofluorescence analysis of retinal sections from DMSO or curcumin-treated *Otud7b*$^{-/-}$ mice after light exposure using an anti-RelA antibody. Nuclei were stained with DAPI.

(K) RelA intensity in the ONL of DMSO or curcumin-treated *Otud7b*$^{-/-}$ mice after light exposure was measured. RelA signal intensity in the ONL decreased in the curcumin-treated *Otud7b*$^{-/-}$ retina. Data are presented as the mean ± SD. *p < 0.05 (unpaired t-test). n = 4 experiments.

OS, outer segment; ONL, outer nuclear layer; INL, inner nuclear layer; GCL, ganglion cell layer.

We found that RelA, a member of the NF-κB family of transcription factors, was activated in the *Otud7b*$^{-/-}$ mouse retina that underwent light-induced damage. The IPA networks also predicted the upregulation of RelB, another NF-κB family transcription factor, as a result of RelA activation. For this reason, we focused on NF-κB for further experiments. In addition, we confirmed that NF-κB activity was upregulated by *Otud7b* knockdown in Neuro2A cells that had undergone serum starvation using a luciferase reporter assay. Furthermore, we showed that inhibition of NF-κB reduced neuronal cell death and photoreceptor damage resulting from *Otud7b* deficiency. While previous studies showed that several compounds suppressed the NF-κB pathway and ameliorated retinal damage,[44–46] the causal relationship between the suppression of the NF-κB pathway and the amelioration of retinal damage has not been investigated. Furthermore, it is not clear in which retinal cell types inhibition of NF-κB can suppress photoreceptor degeneration. We observed that Otud7b is predominantly expressed in photoreceptor cells of the retina, strongly suggesting that the degeneration of photoreceptor cells observed in *Otud7b*$^{-/-}$ retinas under stress is induced by the activated NF-κB pathway in retinal photoreceptor cells. However, we cannot exclude the possibility that NF-κB signaling pathway activation in other retinal cell types lacking *Otud7b* contributes to promoting retinal photoreceptor degeneration. It would be helpful to evaluate the effects of *Otud7b* loss in rod and/or cone photoreceptor cells on retinal damage under stress using conditional approaches, such as the Cre/*loxP* system.

Immunohistochemical analysis showed that Otud7b is expressed in both rod and cone photoreceptor cells. Why are cone photoreceptor cells more damaged than rod photoreceptor cells because of *Otud7b* deficiency under stress conditions? The first possibility is the difference in the expression levels of Otud7b between rod and cone photoreceptor cells. A previous comprehensive transcriptomic analysis showed that Otud7b expression is increased in the *Nrl*$^{-/-}$ mouse retina in which the absence of rod photoreceptor cells is accompanied by an increase in S-cone-like cells,[47,48] suggesting that Otud7b is more highly expressed in cone photoreceptor cells than in rod photoreceptor cells. A second possibility is that cone photoreceptor cells may have increased activation of NF-κB compared with rod photoreceptor cells, resulting in further degradation. We previously performed a microarray analysis of a wild-type mouse retina and *Samd7*$^{-/-}$ mouse retina, in which deletion of *Samd7* caused rod photoreceptor cells to express cone genes.[49] We found that rod-enriched genes were downregulated in the *Samd7*$^{-/-}$ mouse retina, while cone-enriched genes were upregulated in the *Samd7*$^{-/-}$ mouse retina.[49] *Nfkb1*, a gene that encodes the NF-κB family transcription factor p105, was reported to be one of the cone-enriched genes that were upregulated in the *Samd7*$^{-/-}$ mouse retina.[49] In addition, another microarray analysis showed that *Nfkb1* expression increased in the *Nrl*$^{-/-}$ mouse retina from P2 to 2M.[50] *Nfkb1* expression increase was corroborated by other studies that performed RNA-seq analysis on the *Nrl*$^{-/-}$ mouse retina.[51,52] These previous studies suggest that the expression level of *Nfkb1* in cone photoreceptor cells is higher than that in rod photoreceptor cells. When the canonical NF-κB pathway is triggered, p105 undergoes partial degradation and generates p50, which forms dimers with the other NF-κB family transcription factor, translocates to the nucleus, and transactivates NF-κB target genes.[21] Taken together, we speculate that the enriched expression of *Nfkb1* in cone photoreceptor cells results in increased NF-κB activity, leading to greater degeneration than that in rod photoreceptor cells. A third possibility is that the additional deubiquitinase suppresses rod photoreceptor degeneration. Several comprehensive transcriptomic analyses have shown that the expression of *Tnfaip3*, also known as *Otud7c*, is reduced in *Nrl*$^{-/-}$ retina,[51–53] suggesting that the expression level of *Tnfaip3* in rod photoreceptor cells is higher than that in cone photoreceptor cells. In addition, Tnfaip3 is an anti-inflammatory protein that negatively regulates the NF-κB pathway by deubiquitinating RIP1 kinase or TRAF6.[54,55] Thus, Tnfaip3 in addition to Otud7b may suppress rod photoreceptor degeneration through the inhibition of the NF-κB pathway.

Otud7b was independently identified as a negative regulator of the noncanonical NF-κB pathway as it prevents the degradation of TRAF3[56] and of the canonical NF-κB pathway through deubiquitination of RIP1 kinase or TRAF6.[57–59] Under the steady-state, TRAF3 binds to NF-κB-inducing kinase (NIK), resulting in the ubiquitination and degradation of NIK.[19–21,56] Activation of the noncanonical pathway leads to TRAF3 proteolysis, which allows for NIK accumulation. Accumulation of NIK induces phosphorylation of the inhibitor of kappa-B kinase α (IKKα), leading to the ubiquitination and processing of p100.[19–21,56] The inactive precursor protein p100 undergoes proteasome-mediated processing to generate active protein p52, which binds to RelB and translocates to the nucleus.[19–21] The deubiquitination of TRAF3 by Otud7b inhibits NF-κB activation by preventing TRAF3 proteolysis and NIK accumulation.[56] Alternatively, the canonical pathway relies on

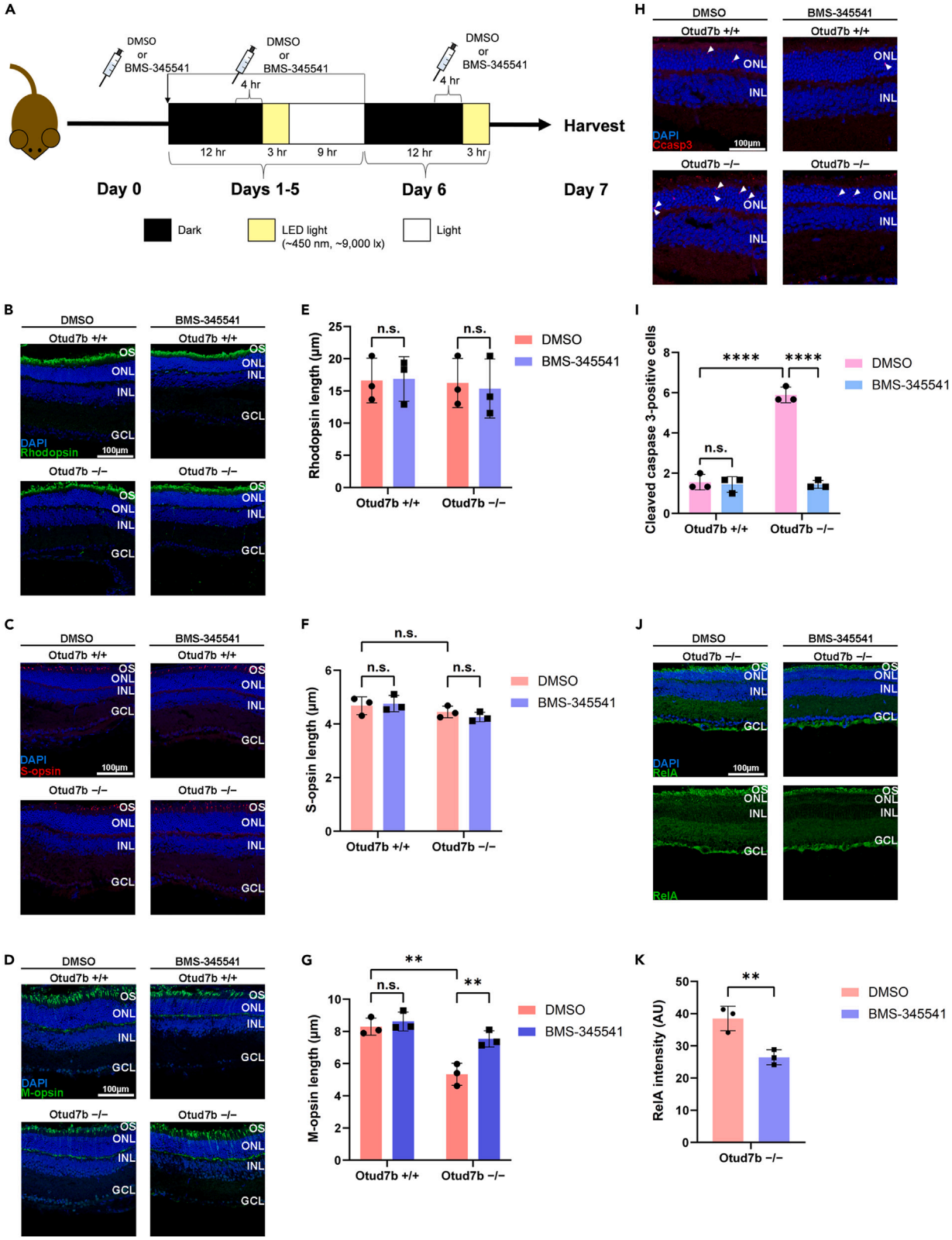
A
DMSO or BMS-345541
DMSO or BMS-345541
DMSO or BMS-345541
4 hr
4 hr
12 hr
3 hr
9 hr
12 hr
3 hr
Harvest
Day 0
Days 1-5
Day 6
Day 7
Dark
LED light (~450 nm, ~9,000 lx)
Light
H
DMSO
BMS-345541
Otud7b +/+
Otud7b −/−
ONL
INL
DAPI
Dcasp3
100μm
B
DMSO
BMS-345541
Otud7b +/+
Otud7b −/−
OS
ONL
INL
GCL
DAPI
Rhodopsin
100μm
E
Rhodopsin length (μm)
n.s.
DMSO
BMS-345541
Otud7b +/+
Otud7b −/−
I
Cleaved caspase 3-positive cells
****
n.s.
DMSO
BMS-345541
C
S-opsin
F
S-opsin length (μm)
J
RelA
D
M-opsin
G
M-opsin length (μm)
**
K
RelA intensity (AU)

Figure 8. NF-κB pathway inhibition by BMS-345541 suppresses light-induced retinal damage in *Otud7b*$^{-/-}$ mice

(A) Schematic representation of LED light exposure to mice treated with BMS-345541. BMS-345541 was injected into mice every day for 7 days.

(B–D) Immunofluorescence analysis of retinal sections from BMS-345541-treated *Otud7b*$^{+/+}$ and *Otud7b*$^{-/-}$ mice after light exposure using the following antibodies: Rhodopsin (a marker for rod outer segments, B), S-opsin (a marker for S-cone outer segments, C), and M-opsin (a marker for M-cone outer segments, D). Nuclei were stained with DAPI.

(E–G) Rod outer segment (E), S-cone outer segment (F), and M-cone outer segment (G) lengths measured in BMS-345541-treated *Otud7b*$^{+/+}$ and *Otud7b*$^{-/-}$ mice after light exposure. The M-cone outer segments were longer in BMS-345541-treated *Otud7b*$^{-/-}$ retina compared to DMSO-treated *Otud7b*$^{-/-}$ retina. *$p < 0.05$, n.s. not significant (two-way ANOVA followed by Tukey's multiple comparisons test), n = 3 per genotype.

(H) Immunofluorescence analysis of retinal sections from BMS-345541-treated *Otud7b*$^{+/+}$ and *Otud7b*$^{-/-}$ mice after light exposure using anti-cleaved caspase 3 antibody. Nuclei were stained with DAPI. White arrows indicate cleaved caspase 3-positive cells.

(I) The number of cleaved caspase 3-positive cells was counted. BMS-345541 treatment significantly reduced the number of cleaved caspase 3-positive cells in the *Otud7b*$^{-/-}$ retina. ****$p < 0.0001$, n.s. not significant (two-way ANOVA followed by Tukey's multiple comparisons test), n = 3 per genotype.

(J) Immunofluorescence analysis of retinal sections from DMSO or BMS-345541-treated *Otud7b*$^{-/-}$ mice after light exposure using an anti-RelA antibody. Nuclei were stained with DAPI.

(K) RelA intensity in the ONL of DMSO or BMS-345541-treated *Otud7b*$^{-/-}$ mice after light exposure was measured. RelA intensity decreased in the BMS-345541-treated Data are presented as the mean ± SD. **$p < 0.01$ (unpaired t-test). n = 3 experiments.

OS, outer segment; ONL, outer nuclear layer; INL, inner nuclear layer; GCL, ganglion cell layer.

ubiquitination of RIP1 kinase or TRAF6. RIP1 and TRAF6 ubiquitination promotes the activation of TAK1, which phosphorylates and activates the inhibitor of kappa-B kinase (IKK).[19–21,57–59] IKK activation triggers phosphorylation of IκBα, resulting in IκBα degradation. Then, the dimer p50/RelA, which is bound to IκBα, is released for nuclear translocation.[19–21,57–59] Otud7b inhibits the activation of NF-κB by deubiquitinating RIP1 kinase and TRAF6.[19–21,57–59] In addition, TRAF3 was reported to suppress the canonical NF-κB pathway in the *Traf3*-deficient mouse thymus.[60] Collectively, these previous reports support the idea that the loss of *Otud7b* can activate both canonical and noncanonical NF-κB pathways in retinal photoreceptor cells.

Limitations of the study

We cannot exclude the possibility that Otud7b is involved in other signaling pathway(s). It was previously reported that Otud7b is a deubiquitinase that deubiquitinates and stabilizes Sox2 and promotes the maintenance of neural progenitor cells.[61] *Otud7b* silencing decreases Sox2 levels and promotes neuronal differentiation in cultured cells. Several studies have revealed that Sox2 is expressed in Müller glia and a subset of amacrine cells in the adult vertebrate retina.[62–64] In addition, the fate determination of retinal progenitor cells depends on the levels of Sox2.[62] Specifically, a decrease in Sox2 levels results in thinning of the retina and loss of ganglion cells, suggesting that the reduction in Sox2 expression results in defective retinal development.[62] However, we did not observe any gross abnormalities in *Otud7b*$^{-/-}$ mouse retinas under normal conditions. Our results imply that Otud7b is not crucial for Sox2 expression in the retina. Defects in the maintenance of neural progenitor cells caused by the loss of Otud7b function may be compensated *in vivo*. Another pathway possibly affected by *Otud7b* deficiency in the retina may be the mTOR pathway. mTOR is the catalytic subunit of two complexes, mTORC1 and mTORC2.[65] mTORC1 comprises mTOR, a regulatory protein associated with mTOR (Raptor) and mammalian lethal with Sec13 protein 8 (mLST8, also referred to as GβL).[65] In contrast, mTORC2 comprises mTOR, rapamycin insensitive companion of mTOR (Rictor), and GβL.[65] Otud7b has been reported to promote mTORC2 signaling through the deubiquitination of GβL.[66] The deletion of *Otud7b* in mouse embryonic fibroblasts elevates mTORC1 formation while reducing mTORC2 formation, resulting in impaired activation of mTORC2 signaling.[66] Notably, loss of *Raptor* accelerates cone death in a mouse model of RP; however, loss of *Rictor* does not affect cone death in that model.[67] Taken together, GβL does not seem to be a functional substrate of Otud7b in the retina. Future studies identifying the target proteins of Otud7b in the retina would deepen our understanding of the molecular mechanisms underlying cone photoreceptor cell protection in retinal degenerative diseases, including AMD and RP, and lead to the development of therapeutic strategies to treat these diseases.

STAR★METHODS

Detailed methods are provided in the online version of this paper and include the following:

- KEY RESOURCES TABLE
- RESOURCE AVAILABILITY
  - Lead contact
  - Materials availability
  - Data and code availability
- EXPERIMENTAL MODEL AND STUDY PARTICIPANT DETAILS
  - Animal care
  - Cell lines
- METHOD DETAILS
  - Generation of *Otud7b*$^{-/-}$ mice
  - Plasmid construction

- Chemicals
- Drug administration
- Cell culture and transfection
- RT-PCR analysis
- Immunofluorescence analysis of retinal sections and cells
- Exposure to LED light
- ERG recordings
- Western blotting
- Cell viability
- RNA-seq and data analysis
- Luciferase reporter assay

- QUANTIFICATION AND STATISTICAL ANALYSIS

SUPPLEMENTAL INFORMATION

Supplemental information can be found online at https://doi.org/10.1016/j.isci.2024.109380.

ACKNOWLEDGMENTS

We thank Dr. Y. Shinkai for the *Mak*$^{-/-}$ mouse, M. Kadowaki, A. Tani, M. Wakabayashi, K. Yoshida, and S. Okochi for technical assistance, and Editage for English language editing. This work was supported by Grant-in-Aid for Scientific Research (21H02657, 20K07326) and Grant-in-Aid for Challenging Research (Exploratory) (23K18199) from the Japan Society for the Promotion of Science, AMED-CREST (21gm1510006) from the Japan Agency for Medical Research and Development, Japan Science and Technology Agency (JST) Moonshot R&D (JPMJMS2024), JST COI-NEXT (JPMJPF2018), The Takeda Science Foundation, and The Uehara Memorial Foundation.

AUTHOR CONTRIBUTIONS

T.C. and T.F. designed the project. T.C., R.T., T.T., and T.F. generated *Otud7b*$^{-/-}$ mice. L.R.V., T.C., Y.M., R.T., S.Z., and T.F. performed histological and molecular biological experiments. L.R.V., T.C., and Y.M. carried out cell culture and biochemical experiments. L.R.V., T.C., and S.Z. performed ERG experiments. L.R.V., T.C., and S.Z. performed light-induced damage experiments. L.R.V., T.C., and D.O. performed RNA-seq experiments. L.R.V., T.C., and T.F. wrote the manuscript. T.F. supervised the project.

DECLARATION OF INTERESTS

The authors declare that they have no conflict of interest.

Received: September 5, 2023
Revised: January 15, 2024
Accepted: February 27, 2024
Published: March 1, 2024

REFERENCES

1. Hartong, D.T., Berson, E.L., and Dryja, T.P. (2006). Retinitis pigmentosa. Lancet *368*, 1795–1809. https://doi.org/10.1016/S0140-6736(06)69740-7.
2. Hamel, C. (2006). Retinitis pigmentosa. Orphanet J. Rare Dis. *1*, 40. https://doi.org/10.1186/1750-1172-1-40.
3. Gagliardi, G., Ben M'Barek, K., and Goureau, O. (2019). Photoreceptor cell replacement in macular degeneration and retinitis pigmentosa: A pluripotent stem cell-based approach. Prog. Retin. Eye Res. *71*, 1–25. https://doi.org/10.1016/j.preteyeres.2019.03.001.
4. Wong, W.L., Su, X., Li, X., Cheung, C.M.G., Klein, R., Cheng, C.Y., and Wong, T.Y. (2014). Global prevalence of age-related macular degeneration and disease burden projection for 2020 and 2040: a systematic review and meta-analysis. Lancet. Glob. Health *2*, e106–e116. https://doi.org/10.1016/S2214-109X(13)70145-1.
5. Milam, A.H., Li, Z.Y., and Fariss, R.N. (1998). Histopathology of the human retina in retinitis pigmentosa. Prog. Retin. Eye Res. *17*, 175–205. https://doi.org/10.1016/s1350-9462(97)00012-8.
6. Song, D.J., Bao, X.L., Fan, B., and Li, G.Y. (2023). Mechanism of Cone Degeneration in Retinitis Pigmentosa. Cell. Mol. Neurobiol. *43*, 1037–1048. https://doi.org/10.1007/s10571-022-01243-2.
7. Johnson, P.T., Lewis, G.P., Talaga, K.C., Brown, M.N., Kappel, P.J., Fisher, S.K., Anderson, D.H., and Johnson, L.V. (2003). Drusen-associated degeneration in the retina. Invest. Ophthalmol. Vis. Sci. *44*, 4481–4488. https://doi.org/10.1167/iovs.03-0436.
8. Justilien, V., Pang, J.J., Renganathan, K., Zhan, X., Crabb, J.W., Kim, S.R., Sparrow, J.R., Hauswirth, W.W., and Lewin, A.S. (2007). SOD2 knockdown mouse model of early AMD. Invest. Ophthalmol. Vis. Sci. *48*, 4407–4420. https://doi.org/10.1167/iovs.07-0432.
9. Rakoczy, P.E., Zhang, D., Robertson, T., Barnett, N.L., Papadimitriou, J., Constable, I.J., and Lai, C.M. (2002). Progressive age-related changes similar to age-related macular degeneration in a transgenic mouse model. Am. J. Pathol. *161*, 1515–1524. https://doi.org/10.1016/S0002-9440(10)64427-6.
10. Elizabeth Rakoczy, P., Yu, M.J.T., Nusinowitz, S., Chang, B., and Heckenlively, J.R. (2006). Mouse models of age-related macular degeneration. Exp. Eye Res. *82*, 741–752. https://doi.org/10.1016/j.exer.2005.10.012.
11. Elsner, A.E., Papay, J.A., Johnston, K.D., Sawides, L., de Castro, A., King, B.J., Jones, D.W., Clark, C.A., Gast, T.J., and Burns, S.A. (2020). Cones in ageing and harsh environments: the neural economy hypothesis. Ophthalmic Physiol. Opt. *40*, 88–116. https://doi.org/10.1111/opo.12670.
12. Baraas, R.C., Horjen, Å., Gilson, S.J., and Pedersen, H.R. (2021). The Relationship Between Perifoveal L-Cone Isolating Visual

Acuity and Cone Photoreceptor Spacing-Understanding the Transition Between Healthy Aging and Early AMD. Front. Aging Neurosci. *13*, 732287. https://doi.org/10.3389/fnagi.2021.732287.
13. Li, Z.Y., Kljavin, I.J., and Milam, A.H. (1995). Rod photoreceptor neurite sprouting in retinitis pigmentosa. J. Neurosci. *15*, 5429–5438. https://doi.org/10.1523/JNEUROSCI.15-08-05429.1995.
14. Lassoued, A., Zhang, F., Kurokawa, K., Liu, Y., Bernucci, M.T., Crowell, J.A., and Miller, D.T. (2021). Cone photoreceptor dysfunction in retinitis pigmentosa revealed by optoretinography. Proc. Natl. Acad. Sci. USA *118*, e2107444118. https://doi.org/10.1073/pnas.2107444118.
15. Brunet, A.A., Harvey, A.R., and Carvalho, L.S. (2022). Primary and Secondary Cone Cell Death Mechanisms in Inherited Retinal Diseases and Potential Treatment Options. Int. J. Mol. Sci. *23*, 726. https://doi.org/10.3390/ijms23020726.
16. Newton, F., and Megaw, R. (2020). Mechanisms of Photoreceptor Death in Retinitis Pigmentosa. Genes *11*, 1120. https://doi.org/10.3390/genes11101120.
17. Mitchell, P., Liew, G., Gopinath, B., and Wong, T.Y. (2018). Age-related macular degeneration. Lancet *392*, 1147–1159. https://doi.org/10.1016/S0140-6736(18)31550-2.
18. Gilmore, T.D. (1999). The Rel/NF-kappaB signal transduction pathway: introduction. Oncogene *18*, 6842–6844. https://doi.org/10.1038/sj.onc.1203237.
19. Hayden, M.S., West, A.P., and Ghosh, S. (2006). NF-kappaB and the immune response. Oncogene *25*, 6758–6780. https://doi.org/10.1038/sj.onc.1209943.
20. Yu, H., Lin, L., Zhang, Z., Zhang, H., and Hu, H. (2020). Targeting NF-kappaB pathway for the therapy of diseases: mechanism and clinical study. Signal Transduct. Target. Ther. *5*, 209. https://doi.org/10.1038/s41392-020-00312-6.
21. Sun, S.C. (2017). The non-canonical NF-kappaB pathway in immunity and inflammation. Nat. Rev. Immunol. *17*, 545–558. https://doi.org/10.1038/nri.2017.52.
22. Mercurio, F., and Manning, A.M. (1999). NF-kappaB as a primary regulator of the stress response. Oncogene *18*, 6163–6171. https://doi.org/10.1038/sj.onc.1203174.
23. Khandelwal, N., Simpson, J., Taylor, G., Rafique, S., Whitehouse, A., Hiscox, J., and Stark, L.A. (2011). Nucleolar NF-kappaB/RelA mediates apoptosis by causing cytoplasmic relocalization of nucleophosmin. Cell Death Differ. *18*, 1889–1903. https://doi.org/10.1038/cdd.2011.79.
24. Zeng, H.Y., Tso, M.O.M., Lai, S., and Lai, H. (2008). Activation of nuclear factor-kappaB during retinal degeneration in rd mice. Mol. Vis. *14*, 1075–1080.
25. Wu, T., Chen, Y., Chiang, S.K.S., and Tso, M.O.M. (2002). NF-kappaB activation in light-induced retinal degeneration in a mouse model. Invest. Ophthalmol. Vis. Sci. *43*, 2834–2840.
26. Chaya, T., Tsutsumi, R., Varner, L.R., Maeda, Y., Yoshida, S., and Furukawa, T. (2019). Cul3-Klhl18 ubiquitin ligase modulates rod transducin translocation during light-dark adaptation. EMBO J. *38*, e101409. https://doi.org/10.15252/embj.2018101409.
27. Nishida, A., Furukawa, A., Koike, C., Tano, Y., Aizawa, S., Matsuo, I., and Furukawa, T. (2003). Otx2 homeobox gene controls retinal photoreceptor cell fate and pineal gland development. Nat. Neurosci. *6*, 1255–1263. https://doi.org/10.1038/nn1155.
28. Omori, Y., Katoh, K., Sato, S., Muranishi, Y., Chaya, T., Onishi, A., Minami, T., Fujikado, T., and Furukawa, T. (2011). Analysis of transcriptional regulatory pathways of photoreceptor genes by expression profiling of the Otx2-deficient retina. PLoS One *6*, e19685. https://doi.org/10.1371/journal.pone.0019685.
29. Tanito, M., Kaidzu, S., Ohira, A., and Anderson, R.E. (2008). Topography of retinal damage in light-exposed albino rats. Exp. Eye Res. *87*, 292–295. https://doi.org/10.1016/j.exer.2008.06.002.
30. Li, T., Snyder, W.K., Olsson, J.E., and Dryja, T.P. (1996). Transgenic mice carrying the dominant rhodopsin mutation P347S: evidence for defective vectorial transport of rhodopsin to the outer segments. Proc. Natl. Acad. Sci. USA *93*, 14176–14181. https://doi.org/10.1073/pnas.93.24.14176.
31. Chrysostomou, V., Stone, J., Stowe, S., Barnett, N.L., and Valter, K. (2008). The status of cones in the rhodopsin mutant P23H-3 retina: light-regulated damage and repair in parallel with rods. Invest. Ophthalmol. Vis. Sci. *49*, 1116–1125. https://doi.org/10.1167/iovs.07-1158.
32. Menghini, M., Jolly, J.K., Nanda, A., Wood, L., Cehajic-Kapetanovic, J., and MacLaren, R.E. (2021). Early Cone Photoreceptor Outer Segment Length Shortening in RPGR X-Linked Retinitis Pigmentosa. Ophthalmologica *244*, 281–290. https://doi.org/10.1159/000507484.
33. Tanimoto, N., Sothilingam, V., Kondo, M., Biel, M., Humphries, P., and Seeliger, M.W. (2015). Electroretinographic assessment of rod- and cone-mediated bipolar cell pathways using flicker stimuli in mice. Sci. Rep. *5*, 10731. https://doi.org/10.1038/srep10731.
34. Omori, Y., Chaya, T., Katoh, K., Kajimura, N., Sato, S., Muraoka, K., Ueno, S., Koyasu, T., Kondo, M., and Furukawa, T. (2010). Negative regulation of ciliary length by ciliary male germ cell-associated kinase (Mak) is required for retinal photoreceptor survival. Proc. Natl. Acad. Sci. USA *107*, 22671–22676. https://doi.org/10.1073/pnas.1009437108.
35. Chaya, T., and Furukawa, T. (2021). Post-translational modification enzymes as key regulators of ciliary protein trafficking. J. Biochem. *169*, 633–642. https://doi.org/10.1093/jb/mvab024.
36. Tucker, B.A., Scheetz, T.E., Mullins, R.F., DeLuca, A.P., Hoffmann, J.M., Johnston, R.M., Jacobson, S.G., Sheffield, V.C., and Stone, E.M. (2011). Exome sequencing and analysis of induced pluripotent stem cells identify the cilia-related gene male germ cell-associated kinase (MAK) as a cause of retinitis pigmentosa. Proc. Natl. Acad. Sci. USA *108*, E569–E576. https://doi.org/10.1073/pnas.1108918108.
37. Ozgül, R.K., Siemiatkowska, A.M., Yücel, D., Myers, C.A., Collin, R.W.J., Zonneveld, M.N., Beryozkin, A., Banin, E., Hoyng, C.B., van den Born, L.I., et al. (2011). Exome sequencing and cis-regulatory mapping identify mutations in MAK, a gene encoding a regulator of ciliary length, as a cause of retinitis pigmentosa. Am. J. Hum. Genet. *89*, 253–264. https://doi.org/10.1016/j.ajhg.2011.07.005.
38. Lee, S.B., Kim, J.J., Kim, T.W., Kim, B.S., Lee, M.S., and Yoo, Y.D. (2010). Serum deprivation-induced reactive oxygen species production is mediated by Romo1. Apoptosis *15*, 204–218. https://doi.org/10.1007/s10495-009-0411-1.
39. White, E.Z., Pennant, N.M., Carter, J.R., Hawsawi, O., Odero-Marah, V., and Hinton, C.V. (2020). Serum deprivation initiates adaptation and survival to oxidative stress in prostate cancer cells. Sci. Rep. *10*, 12505. https://doi.org/10.1038/s41598-020-68668-x.
40. Caamaño, J., and Hunter, C.A. (2002). NF-kappaB family of transcription factors: central regulators of innate and adaptive immune functions. Clin. Microbiol. Rev. *15*, 414–429. https://doi.org/10.1128/CMR.15.3.414-429.2002.
41. Oeckinghaus, A., and Ghosh, S. (2009). The NF-kappaB family of transcription factors and its regulation. Cold Spring Harb. Perspect. Biol. *1*, a000034. https://doi.org/10.1101/cshperspect.a000034.
42. Warwick, R.A., Kaushansky, N., Sarid, N., Golan, A., and Rivlin-Etzion, M. (2018). Inhomogeneous Encoding of the Visual Field in the Mouse Retina. Curr. Biol. *28*, 655–665.e3. https://doi.org/10.1016/j.cub.2018.01.016.
43. Ranchon, I., LaVail, M.M., Kotake, Y., and Anderson, R.E. (2003). Free radical trap phenyl-N-tert-butylnitrone protects against light damage but does not rescue P23H and S334ter rhodopsin transgenic rats from inherited retinal degeneration. J. Neurosci. *23*, 6050–6057. https://doi.org/10.1523/JNEUROSCI.23-14-06050.2003.
44. Kim, J., Jin, H.L., Jang, D.S., Jeong, K.W., and Choung, S.Y. (2018). Quercetin-3-O-alpha-l-arabinopyranoside protects against retinal cell death via blue light-induced damage in human RPE cells and Balb-c mice. Food Funct. *9*, 2171–2183. https://doi.org/10.1039/c7fo01958k.
45. Wang, K., Xiao, J., Peng, B., Xing, F., So, K.F., Tipoe, G.L., and Lin, B. (2014). Retinal structure and function preservation by polysaccharides of wolfberry in a mouse model of retinal degeneration. Sci. Rep. *4*, 7601. https://doi.org/10.1038/srep07601.
46. Cho, H.M., Lee, S.J., and Choung, S.Y. (2023). Protective effects of Panax ginseng berry extract on blue light-induced retinal damage in ARPE-19 cells and mouse retina. J. Ginseng Res. *47*, 65–73. https://doi.org/10.1016/j.jgr.2022.04.002.
47. Mears, A.J., Kondo, M., Swain, P.K., Takada, Y., Bush, R.A., Saunders, T.L., Sieving, P.A., and Swaroop, A. (2001). Nrl is required for rod photoreceptor development. Nat. Genet. *29*, 447–452. https://doi.org/10.1038/ng774.
48. Esquerdo-Barragán, M., Brooks, M.J., Toulis, V., Swaroop, A., and Marfany, G. (2019). Expression of deubiquitinating enzyme genes in the developing mammal retina. Mol. Vis. *25*, 800–813.
49. Omori, Y., Kubo, S., Kon, T., Furuhashi, M., Narita, H., Kominami, T., Ueno, A., Tsutsumi, R., Chaya, T., Yamamoto, H., et al. (2017). Samd7 is a cell type-specific PRC1 component essential for establishing retinal rod photoreceptor identity. Proc. Natl. Acad. Sci. USA *114*, E8264–E8273. https://doi.org/10.1073/pnas.1707021114.
50. Mo, A., Luo, C., Davis, F.P., Mukamel, E.A., Henry, G.L., Nery, J.R., Urich, M.A., Picard, S., Lister, R., Eddy, S.R., et al. (2016). Epigenomic landscapes of retinal rods and cones. Elife *5*, e11613. https://doi.org/10.7554/eLife.11613.
51. Brooks, M.J., Rajasimha, H.K., Roger, J.E., and Swaroop, A. (2011). Next-generation sequencing facilitates quantitative analysis of

wild-type and Nrl(-/-) retinal transcriptomes. Mol. Vis. *17*, 3034–3054.
52. Yoshida, S., Mears, A.J., Friedman, J.S., Carter, T., He, S., Oh, E., Jing, Y., Farjo, R., Fleury, G., Barlow, C., et al. (2004). Expression profiling of the developing and mature Nrl-/- mouse retina: identification of retinal disease candidates and transcriptional regulatory targets of Nrl. Hum. Mol. Genet. *13*, 1487–1503. https://doi.org/10.1093/hmg/ddh160.
53. Kim, J.W., Yang, H.J., Brooks, M.J., Zelinger, L., Karakülah, G., Gotoh, N., Boleda, A., Gieser, L., Giuste, F., Whitaker, D.T., et al. (2016). NRL-Regulated Transcriptome Dynamics of Developing Rod Photoreceptors. Cell Rep. *17*, 2460–2473. https://doi.org/10.1016/j.celrep.2016.10.074.
54. Sun, S.C. (2008). Deubiquitylation and regulation of the immune response. Nat. Rev. Immunol. *8*, 501–511. https://doi.org/10.1038/nri2337.
55. Catrysse, L., Vereecke, L., Beyaert, R., and van Loo, G. (2014). A20 in inflammation and autoimmunity. Trends Immunol. *35*, 22–31. https://doi.org/10.1016/j.it.2013.10.005.
56. Hu, H., Brittain, G.C., Chang, J.H., Puebla-Osorio, N., Jin, J., Zal, A., Xiao, Y., Cheng, X., Chang, M., Fu, Y.X., et al. (2013). OTUD7B controls non-canonical NF-kappaB activation through deubiquitination of TRAF3. Nature *494*, 371–374. https://doi.org/10.1038/nature11831.
57. Enesa, K., Zakkar, M., Chaudhury, H., Luong, L.A., Rawlinson, L., Mason, J.C., Haskard, D.O., Dean, J.L.E., and Evans, P.C. (2008). NF-kappaB suppression by the deubiquitinating enzyme Cezanne: a novel negative feedback loop in pro-inflammatory signaling. J. Biol. Chem. *283*, 7036–7045. https://doi.org/10.1074/jbc.M708690200.
58. Ji, Y., Cao, L., Zeng, L., Zhang, Z., Xiao, Q., Guan, P., Chen, S., Chen, Y., Wang, M., and Guo, D. (2018). The N-terminal ubiquitin-associated domain of Cezanne is crucial for its function to suppress NF-kappaB pathway. J. Cell. Biochem. *119*, 1979–1991. https://doi.org/10.1002/jcb.26359.
59. Luong, L.A., Fragiadaki, M., Smith, J., Boyle, J., Lutz, J., Dean, J.L.E., Harten, S., Ashcroft, M., Walmsley, S.R., Haskard, D.O., et al. (2013). Cezanne regulates inflammatory responses to hypoxia in endothelial cells by targeting TRAF6 for deubiquitination. Circ. Res. *112*, 1583–1591. https://doi.org/10.1161/CIRCRESAHA.111.300119.
60. Zarnegar, B., Yamazaki, S., He, J.Q., and Cheng, G. (2008). Control of canonical NF-kappaB activation through the NIK-IKK complex pathway. Proc. Natl. Acad. Sci. USA *105*, 3503–3508. https://doi.org/10.1073/pnas.0707959105.
61. Cui, C.P., Zhang, Y., Wang, C., Yuan, F., Li, H., Yao, Y., Chen, Y., Li, C., Wei, W., Liu, C.H., et al. (2018). Dynamic ubiquitylation of Sox2 regulates proteostasis and governs neural progenitor cell differentiation. Nat. Commun. *9*, 4648. https://doi.org/10.1038/s41467-018-07025-z.
62. Taranova, O.V., Magness, S.T., Fagan, B.M., Wu, Y., Surzenko, N., Hutton, S.R., and Pevny, L.H. (2006). SOX2 is a dose-dependent regulator of retinal neural progenitor competence. Genes Dev. *20*, 1187–1202. https://doi.org/10.1101/gad.1407906.
63. Surzenko, N., Crowl, T., Bachleda, A., Langer, L., and Pevny, L. (2013). SOX2 maintains the quiescent progenitor cell state of postnatal retinal Muller glia. Development *140*, 1445–1456. https://doi.org/10.1242/dev.071878.
64. Lin, Y.P., Ouchi, Y., Satoh, S., and Watanabe, S. (2009). Sox2 plays a role in the induction of amacrine and Muller glial cells in mouse retinal progenitor cells. Invest. Ophthalmol. Vis. Sci. *50*, 68–74. https://doi.org/10.1167/iovs.07-1619.
65. Melick, C.H., and Jewell, J.L. (2020). Regulation of mTORC1 by Upstream Stimuli. Genes *11*, 989. https://doi.org/10.3390/genes11090989.
66. Wang, B., Jie, Z., Joo, D., Ordureau, A., Liu, P., Gan, W., Guo, J., Zhang, J., North, B.J., Dai, X., et al. (2017). TRAF2 and OTUD7B govern a ubiquitin-dependent switch that regulates mTORC2 signalling. Nature *545*, 365–369. https://doi.org/10.1038/nature22344.
67. Venkatesh, A., Ma, S., Le, Y.Z., Hall, M.N., Rüegg, M.A., and Punzo, C. (2015). Activated mTORC1 promotes long-term cone survival in retinitis pigmentosa mice. J. Clin. Invest. *125*, 1446–1458. https://doi.org/10.1172/JCI79766.
68. Sato, S., Omori, Y., Katoh, K., Kondo, M., Kanagawa, M., Miyata, K., Funabiki, K., Koyasu, T., Kajimura, N., Miyoshi, T., et al. (2008). Pikachurin, a dystroglycan ligand, is essential for photoreceptor ribbon synapse formation. Nat. Neurosci. *11*, 923–931. https://doi.org/10.1038/nn.2160.
69. Koike, C., Nishida, A., Ueno, S., Saito, H., Sanuki, R., Sato, S., Furukawa, A., Aizawa, S., Matsuo, I., Suzuki, N., et al. (2007). Functional roles of Otx2 transcription factor in postnatal mouse retinal development. Mol. Cell Biol. *27*, 8318–8329. https://doi.org/10.1128/MCB.01209-07.
70. Shinkai, Y., Satoh, H., Takeda, N., Fukuda, M., Chiba, E., Kato, T., Kuramochi, T., and Araki, Y. (2002). A testicular germ cell-associated serine-threonine kinase, MAK, is dispensable for sperm formation. Mol. Cell Biol. *22*, 3276–3280. https://doi.org/10.1128/MCB.22.10.3276-3280.2002.
71. Itoh, Y., Moriyama, Y., Hasegawa, T., Endo, T.A., Toyoda, T., and Gotoh, Y. (2013). Scratch regulates neuronal migration onset via an epithelial-mesenchymal transition-like mechanism. Nat. Neurosci. *16*, 416–425. https://doi.org/10.1038/nn.3336.
72. Cong, L., Ran, F.A., Cox, D., Lin, S., Barretto, R., Habib, N., Hsu, P.D., Wu, X., Jiang, W., Marraffini, L.A., and Zhang, F. (2013). Multiplex genome engineering using CRISPR/Cas systems. Science *339*, 819–823. https://doi.org/10.1126/science.1231143.
73. Chaya, T., Omori, Y., Kuwahara, R., and Furukawa, T. (2014). ICK is essential for cell type-specific ciliogenesis and the regulation of ciliary transport. EMBO J. *33*, 1227–1242. https://doi.org/10.1002/embj.201488175.
74. Irie, S., Sanuki, R., Muranishi, Y., Kato, K., Chaya, T., and Furukawa, T. (2015). Rax Homeoprotein Regulates Photoreceptor Cell Maturation and Survival in Association with Crx in the Postnatal Mouse Retina. Mol. Cell Biol. *35*, 2583–2596. https://doi.org/10.1128/MCB.00048-15.
75. Okamoto, S., Chaya, T., Omori, Y., Kuwahara, R., Kubo, S., Sakaguchi, H., and Furukawa, T. (2017). Ick Ciliary Kinase Is Essential for Planar Cell Polarity Formation in Inner Ear Hair Cells and Hearing Function. J. Neurosci. *37*, 2073–2085. https://doi.org/10.1523/JNEUROSCI.3067-16.2017.
76. Tsutsumi, R., Chaya, T., and Furukawa, T. (2018). Enriched expression of the ciliopathy gene Ick in cell proliferating regions of adult mice. Gene Expr. Patterns *29*, 18–23. https://doi.org/10.1016/j.gep.2018.04.005.
77. Chaya, T., Ishikane, H., Varner, L.R., Sugita, Y., Maeda, Y., Tsutsumi, R., Motooka, D., Okuzaki, D., and Furukawa, T. (2022). Deficiency of the neurodevelopmental disorder-associated gene Cyfip2 alters the retinal ganglion cell properties and visual acuity. Hum. Mol. Genet. *31*, 535–547. https://doi.org/10.1093/hmg/ddab268.
78. Wenzel, A., Reme, C.E., Williams, T.P., Hafezi, F., and Grimm, C. (2001). The Rpe65 Leu450Met variation increases retinal resistance against light-induced degeneration by slowing rhodopsin regeneration. J. Neurosci. *21*, 53–58. https://doi.org/10.1523/JNEUROSCI.21-01-00053.2001.
79. Tsutsumi, R., Chaya, T., Tsujii, T., and Furukawa, T. (2022). The carboxyl-terminal region of SDCCAG8 comprises a functional module essential for cilia formation as well as organ development and homeostasis. J. Biol. Chem. *298*, 101686. https://doi.org/10.1016/j.jbc.2022.101686.
80. Kubo, S., Yamamoto, H., Kajimura, N., Omori, Y., Maeda, Y., Chaya, T., and Furukawa, T. (2021). Functional analysis of Samd11, a retinal photoreceptor PRC1 component, in establishing rod photoreceptor identity. Sci. Rep. *11*, 4180. https://doi.org/10.1038/s41598-021-83781-1.
81. Chaya, T., Maeda, Y., Sugimura, R., Okuzaki, D., Watanabe, S., Varner, L.R., Motooka, D., Gyoten, D., Yamamoto, H., Kato, H., and Furukawa, T. (2022). Multiple knockout mouse and embryonic stem cell models reveal the role of miR-124a in neuronal maturation. J. Biol. Chem. *298*, 102293. https://doi.org/10.1016/j.jbc.2022.102293.

STAR★METHODS

KEY RESOURCES TABLE

REAGENT or RESOURCE	SOURCE	IDENTIFIER
Antibodies		
Mouse monoclonal anti-Rhodopsin	Sigma	Cat#O4886
Mouse monoclonal anti-Pax6	DSHB	Cat# pax6, RRID:AB_528427
Mouse monoclonal anti-S100β	Sigma	Cat#S2532; RRID:AB_477499
Mouse monoclonal anti-Ctbp2	BD Biosciences	Cat#612044; RRID:AB_399431
Rabbit polyclonal anti-*M*-opsin	Millipore	Cat#AB5405; RRID:AB_177456
Rabbit polyclonal anti-Pikachurin	Sato et al.[68]	N/A
Rabbit polyclonal anti-Gnat2	Abcam	Cat#AB97501
Rabbit polyclonal anti-Chx10	Koike et al.[69]	N/A
Rabbit polyclonal anti-Calbindin	Calbiochem	Cat#PC253L
Rabbit polyclonal anti-Otud7b	Proteintech	Cat#16605-1-AP; RRID:AB_2157149
Rabbit polyclonal anti-GFP	MBL	Cat#598; RRID:AB_591816
Rabbit anti-cleaved caspase 3	Cell Signaling	Cat#9661; RRID:AB_2341188
Goat anti-S-opsin	Santa Cruz	Cat#sc-14363; RRID:AB_2158332
Goat anti-S-opsin	ROCKLAND	Cat#600-101-MP7S
Guinea pig polyclonal anti-Rbpms	Millipore	Cat#ABN1376; RRID:AB_2687403
Rhodamine-labeled peanut agglutinin (PNA)	Vector Laboratories	Cat#RL-1072; RRID:AB_2336642
Mouse monoclonal anti-GFAP	Sigma	Cat#G3893-.2ML
Rabbit polyclonal anti-Iba1	WAKO	Cat#019–19741; RRID:AB_839504
Rabbit polyclonal anti-p65	Abcam	Cat#ab16502; RRID:AB_443394
Mouse monoclonal anti-α-Tubulin	Sigma	Cat#T9026; RRID:AB_477593
mouse monoclonal anti-FLAG M2	Sigma	Cat#F1804; RRID:AB_262044
Alexa Fluor 488 anti-mouse IgG	Invitrogen	Cat#A21202; RRID:AB_141607
Alexa Fluor 488 anti-rabbit IgG	Invitrogen	Cat#A21206; RRID:AB_141708
Cy3 anti-mouse IgG	Jackson Laboratory	Cat#715-165-150; RRID:AB_2340813
Cy3 anti-rabbit IgG	Jackson Laboratory	Cat#711-165-152; RRID:AB_2307443
Cy3 anti-goat IgG	Jackson Laboratory	Cat#705-165-147; RRID:AB_2307351
Cy3 anti-guinea pig IgG	Jackson Laboratory	Cat#706-165-148; RRID:AB_2340460
Horseradish peroxidase-conjugated anti-mouse IgG	Zymed	Cat#81-6520
Horseradish peroxidase-conjugated anti-rabbit IgG	Jackson Laboratory	Cat#111-035-144; RRID:AB_2307391
Horseradish peroxidase-conjugated anti-rat IgG	Jackson Laboratory	Cat#112-035-062; RRID:AB_2338133
Chemicals, peptides, and recombinant proteins		
Curcumin	Sigma	Cat#C7727
BMS-345541	Sigma-Aldrich	Cat#B9935-5MG
DAPI (0.1 mg/ml)	Nacalai Tesque	Cat#11034-56
Critical commercial assays		
Invitrogen™ ReadyProbes™ Cell Viability Imaging Kit	Invitrogen	Cat#R37610
Nano-Glo Dual-Luciferase Reporter Assay System	Promega	Cat#N1610
Deposited data		
RNA sequence	This paper	GEO: GSE239573

(*Continued on next page*)

Continued

REAGENT or RESOURCE	SOURCE	IDENTIFIER
Experimental models: Cell lines		
HEK293T cell	RIKEN RCB	Cat#RCB1637
Neuro2A cell	JCRB Cell Bank	Cat#IFO50081
Experimental models: Organisms/strains		
Otud7b$^{-/-}$ mice	This paper	N/A
Mak$^{-/-}$ mice	Shinkai et al.[70]	N/A
Oligonucleotides		
Otud7b-shRNA1: 5′-GTGCTGAGGAAAGCGCTGTAT-3′	This paper	N/A
shRNA-control: 5′-GACGTCTAACGGATTCGAGCT-3′	Itoh et al.[71]	N/A
siGENOME non-targeting siRNA pool #2: UAAGGCUAUGAAGAGAUAC, AUGUAUUGGCCUGUAUUAG, AUGAACGUAGAAUUGCUCAA, and UGGUUUACAUGUCGACUAA	Dharmacon	Cat# D-001206-14-05
siGENOME_mouse_Otud7b: GCCGGUAUAUGAAAGCCUA	Dharmacon	Cat# D-050018-03
siGENOME_mouse_Otud7b: GCAAUGGCGGGAGCAAGUA	Dharmacon	Cat# D-050018-04
minimal promoter: 5′-AGACACTAGAGGG TATATAATGGAAGCTCGACTTCCAG-3′	This paper	N/A
5x NF-κB response element: 5′-GGGAATT TCCGGGGACTTTCCGGGAATTTCCGGG GACTTTCCGGGAATTTCC-3′	This paper	N/A
See Table S1 for CRISPR, genotyping, RT-PCR, construct	This paper	N/A
Recombinant DNA		
pCAGGSII-N-3x-FLAG mouse Otud7b	This paper	N/A
Software and algorithms		
ImageJ	NIH	https://imagej.nih.gov/ij/
GraphPad Prism	GraphPad Software	https://www.graphpad.com
ZEN (Black Edition) Image	Carl Zeiss	https://www.zeiss.com/microscopy/en/home.html; RRID: SCR_018163
Zen (Blue Edition) Image Acquisition	Carl Zeiss	https://www.zeiss.com/microscopy/en/home.html; RRID: SCR_013672

RESOURCE AVAILABILITY

Lead contact

Further information and requests for resources and reagents should be directed to and will be fulfilled by the lead contact, Takahisa Furukawa. E-mail: takahisa.furukawa@protein.osaka-u.ac.jp.

Materials availability

Plasmids and cell lines generated in this study are available upon request.

Data and code availability

- RNA-seq data have been deposited at GEO and are publicly available as of the date of publication. Accession numbers are listed in the key resources table.
- This paper does not report original code.
- Any additional information required to reanalyze the data reported in this paper is available from the lead contact upon request.

EXPERIMENTAL MODEL AND STUDY PARTICIPANT DETAILS

Animal care

All procedures conformed to the ARVO Statement for the Use of Animals in Ophthalmic and Vision Research, and these procedures were approved by the Institutional Safety Committee on Recombinant DNA Experiments (approval ID 04913) and the Animal Experimental Committees of Institute for Protein Research (approval ID R04-02-0), Osaka University, and were performed in compliance with the institutional guidelines. Mice were housed in a temperature-controlled room at 22°C with a 12 h light/dark cycle. Fresh water and rodent diet were available at all times. All animal experiments were performed with mice of either sex at 1 M, 2 M, or 6 M.

Cell lines

HEK293T (RIKEN RCB, RCB1637) and Neuro2A (JCRB Cell Bank, IFO50081) cells were cultured in Dulbecco's modified Eagle's medium (DMEM) containing 10% fetal bovine serum supplemented with penicillin (100 μg/mL) and streptomycin (100 μg/mL) at 37°C with 5% CO_2.

METHOD DETAILS

Generation of *Otud7b*$^{-/-}$ mice

Otud7b$^{-/-}$ mice were generated using the CRISPR/Cas9 system. Two gRNAs were designed within exon 2 of the *Otud7b* gene using CRISPR Design (http://crispr.mit.edu/). Oligo DNAs for the gRNA sequence were cloned into the pX330 vector.[72] The plasmid constructs were co-injected into B6C3F1 fertilized eggs, which were then transferred into the uteri of pseudopregnant ICR females. Mutated individuals were selected using PCR and subjected to sequencing analyses. *Otud7b*$^{-/-}$ mice were crossed with *Mak*$^{-/-}$ mice[70] to generate *Otud7b*$^{-/-}$; *Mak*$^{-/-}$ mice. The primer sequences for the gRNA expression plasmid and genotyping are listed in Table S1.

Plasmid construction

Plasmids expressing enhanced green fluorescent protein (EGFP) have been previously constructed.[34,73] The full-length cDNA fragment of mouse *Otud7b* was amplified by PCR using mouse retinal cDNA as a template and subcloned into the pCAGGSII-N-3xFLAG vector.[74] For *Otud7b* knockdown, the Otud7b-shRNA and shRNA-control cassettes were subcloned into the pBAsi-mU6 vector (Takara Bio). The target sequences were as follows: Otud7b-shRNA1, 5′-GTGCTGAGGAAAGCGCTGTAT-3′ and shRNA-control, 5′-GACGTCTAACGGATTC GAGCT-3′.[71] Primer sequences used for amplification are listed in Table S1.

Chemicals

Curcumin (Sigma, C7727) was dissolved in DMSO at 200 mg/mL or 5 mM and stored at −20°C. BMS-345541 (Sigma-Aldrich, B9935-5MG) was dissolved in DMSO at 25 mg/mL or 50 mM and stored at −20°C.

Drug administration

Curcumin was dissolved in DMSO (200 mg/mL) and diluted with sunflower seed oil (Sigma-Aldrich). Curcumin (100 mg/kg) was administered to the mice daily by subcutaneous injection 4 h before light exposure. BMS-3455341 was dissolved in DMSO (25 mg/mL) and diluted with sunflower seed oil. BMS-345541 (30 mg/kg) was administered to the mice daily by subcutaneous injection 4 h before light exposure.

Cell culture and transfection

Transfection was performed using the calcium phosphate method for HEK293T cells. Neuro2A cell transfection was performed using Lipofectamine 3000 (Thermo Fisher Scientific) for shRNA and Lipofectamine RNAiMAX (Life Technologies) for siRNA. To induce cellular stress in transfected cells, the medium was replaced with a serum-free medium 24 or 48 h after transfection, and the cells were cultured for 14 h in a serum-free medium. To examine the effects of curcumin and BMS-345541 on cellular stress, Neuro2A cells were incubated with serum-supplemented medium containing 5 μM curcumin or 2 μM BMS-345541 for 4 h before and 24 h after transfection and further incubated with serum-free medium containing 5 μM curcumin or 2 μM BMS-345541 for 24 h. For knockdown experiments, the cells were transfected with siGENOME nontargeting siRNA pool #2 or mouse Otud7b siRNA (Dharmacon-Horizon Discovery). The following are the catalog numbers and siRNA sequences: nontargeting control #2, catalog no. D-001206-14-05, target sequences: UAAGGCUAUGAAGAGAUAC, AUGUAUUGG CCUGUAUUAG, AUGAACGUAGAAUUGCUCAA, and UGGUUUACAUGUCGACUAA; siGENOME_ mouse_Otud7b, catalog no. D-050018-03; target sequence: GCCGGUAUAUGAAAGCCUA; siGENOME_mouse_Otud7b, catalog no. D-050018-04; target sequence, GCAAUGGCGGGAGCAAGUA.

RT-PCR analysis

RT-PCR was performed as described previously.[75,76] Total RNA was extracted from tissues dissected from ICR mice at 4 weeks using TRIzol (Ambion). Total RNA (2 μg) was reverse-transcribed into cDNA with random hexamers using PrimescriptII (TaKaRa). Human cDNA was purchased from Clontech (Mountain View, CA, USA). The cDNA was used for PCR with rTaq polymerase (TaKaRa).

Immunofluorescence analysis of retinal sections and cells

Immunofluorescence analysis of retinal sections was performed as described previously.[77] Mouse eyes and eyecups were fixed in 4% paraformaldehyde (PFA) in phosphate-buffered saline (PBS) for 5 or 30 min. Samples were placed in 30% sucrose in PBS overnight at 4°C and embedded in TissueTec OCT Compound 4583 (Sakura). Frozen 20-μm sections placed on slides were dried overnight at room temperature. Tissue sections from eyecups were washed three times with PBS. Eye cryosections were fixed in methanol for 5 min before washing three times with PBS. The samples were then incubated with blocking buffer (5% normal donkey serum and 0.1% Triton X-100 in PBS) for 1 h at room temperature and immunostained with primary antibodies in blocking buffer overnight at 4°C. After washing with PBS, the samples were incubated with fluorescent dye-conjugated secondary antibodies and DAPI (1:1,000, Nacalai Tesque). Neuro2A cells were washed with PBS, fixed with 4% PFA in PBS for 5 min at room temperature, and incubated with blocking buffer for 1 h at room temperature. Cells were immunostained with primary antibodies in blocking buffer overnight at 4°C, washed with PBS, and incubated with fluorescent dye-conjugated secondary antibodies and DAPI in blocking buffer for 2 h at room temperature. The samples were washed three times with PBS and then coverslipped with gelvatol.

The primary antibodies used in this study were as follows: mouse anti-Rhodopsin (1:1,000, Sigma, O4886), mouse anti-Pax6 (1:500, DSHB), mouse anti-S100β (1:200, Sigma, S-2532), mouse anti-Ctbp2 (1:500, BD Biosciences, 612044), rabbit anti-*M*-opsin (1:500, Millipore, AB5405), rabbit anti-Pikachurin (1:300),[68] rabbit anti-Gnat2 (1:500, Abcam, ab97501), rabbit anti-Chx10 (1:200),[69] rabbit anti-Calbindin (1:200, Calbiochem, PC253L), rabbit anti-Otud7b (1:500, Proteintech, 16605-1-AP), rabbit anti-GFP (1:2,500, MBL, 598), rabbit anti-cleaved caspase 3 (1:500, Cell Signaling, 9661), goat anti-S-opsin (1:500, Santa Cruz, sc-14363 or 1:500, ROCKLAND, 600-101-MP7S), rabbit anti-Iba1 (1:500, WAKO, 019–19741), mouse anti-GFAP (1:500, Sigma, G3893-.2ML), and guinea pig anti-Rbpms (1:1,000, Millipore, ABN1376). Cy3-conjugated (1:500; Jackson ImmunoResearch Laboratories) and Alexa Fluor 488-conjugated (1:500; Sigma-Aldrich) secondary antibodies were used. DAPI was used for nuclear staining. The specimens were observed under a laser confocal microscope (LSM700 or LSM900; Carl Zeiss). Rhodamine-labeled peanut agglutinin (PNA) (1:250) (RL-1072, Vector Laboratories) was used to stain cone photoreceptor synapses. The thicknesses and lengths of the ONL, INL+IPL+GCL, M-opsin, S-opsin, and Gnat2 were measured using ZEN imaging software (ZEN (black edition) or ZEN (blue edition), Carl Zeiss).

Exposure to LED light

Exposure to LED light was performed as described previously.[26] Animals were maintained in the dark for 12 h. Thirty minutes before LED light (~450 nm) exposure, the pupils were dilated using 1% cyclopentolate hydrochloride eye drops (Santen Pharmaceuticals, Osaka, Japan). The non-anesthetized mice were exposed to ~9,000 lux LED light for 3 h in a mirrored box with clear partitions to separate the mice while allowing for light reflection. The ambient temperature was maintained at 25 ± 1.5°C during the light exposure. The mice were returned to their cages after light exposure and kept under normal light conditions for 9 h before the next 12 h dark cycle. Light exposure was repeated for 6 days. ERG recordings and/or retinal dissections were performed on day 7. *Otud7b*$^{+/-}$ mice were backcrossed with 129S6/*SvEvTac* mice to generate *Otud7b*$^{+/+}$ and *Otud7b*$^{-/-}$ mice homozygous for the variant encoding Leu450 in the *Rpe65* gene, which was used for the experiment.[78] *Otud7b*$^{+/+}$ and *Otud7b*$^{-/-}$ mice treated with curcumin were also subjected to the experiment.

ERG recordings

Electroretinograms (ERGs) were recorded as described previously.[79] The mice were adapted to the dark overnight. Ketamine (100 mg/kg) and xylazine (10 mg/kg) diluted in saline (Otsuka) were injected intraperitoneally to anesthetize the mice. Pupils were dilated with topical 0.5% tropicamide and 0.5% phenylephrine HCl. The ERG responses were measured using the PuREC system with LED electrodes (Mayo Corporation). Scotopic ERGs were recorded at four stimulus intensities ranging from −4.0 to 1.0 log cd s/m^2. The mice were light-adapted for 10 min before photopic ERGs were recorded on a rod-suppressing white background of 1.3 log cd s/m^2. Photopic ERGs were recorded at four stimulus intensities ranging from −0.5 to 1.0 log cd s/m^2. Eight and four responses were averaged for the scotopic recordings (−4.0 and −3.0 log cd s/m^2, respectively). Sixteen responses were averaged for the photopic recordings.

Western blotting

Western blotting was performed as previously described.[80] Neuro2A cells were washed with PBS twice and lysed in a lysis buffer supplemented with protease inhibitors (buffer A: 20 mM Tris-HCl pH 7.4, 150 mM NaCl, 1% Nonidet P-40, 1 mM EDTA, 1 mM PMSF, 2 μg/mL leupeptin, 5 μg/mL aprotinin, and 3 μg/mL pepstatin A). Mouse retinas were lysed in lysis buffer supplemented protease inhibitors (buffer B: 20 mM Tris-HCl pH 7.4, 150 mM NaCl, 1% Nonidet P-40, 0.5 mM EDTA, 1 mM PMSF, 2 μg/mL leupeptin, 5 μg/mL aprotinin, and 3 μg/mL pepstatin A). Samples were resolved by SDS-PAGE and transferred to PVDF membranes (Millipore) using a semi-dry transfer cell (Bio-Rad) or the iBlot system (Invitrogen). The membranes were blocked with blocking buffer (3% skim milk and 0.05% Tween 20 in Tris-buffered saline (TBS)) for 1 h and incubated with primary antibodies overnight at 4°C. The membranes were washed with 0.05% Tween 20 in TBS three times for 10 min each and then incubated with secondary antibodies for 2–5 h at room temperature. Signals were detected using a Chemi-Lumi One L (Nacalai) or Pierce Western Blotting Substrate Plus (Thermo Fisher Scientific). The following primary antibodies were used: mouse anti-FLAG M2 (1:5,000, Sigma, F1804), mouse anti-α-tubulin (Cell Signaling Technology, DM1A, 1:5,000, T9026), rabbit anti-GFP (1:2,500, MBL, 598), rabbit anti-cleaved caspase 3 (1:100, Cell Signaling, 9661), and rabbit anti-Otud7b (1:500, Proteintech, 16605-1-AP). The following secondary antibodies were used: horseradish peroxidase-conjugated anti-mouse IgG (1:10,000; Zymed) and anti-rabbit IgG (1:10,000; Jackson Laboratory).

Cell viability

Neuro2A cells transfected with shRNA or siRNA were cultured in serum-free medium for 14 h. Viability was assayed using a ReadyProbes Cell Viability Imaging Kit (Blue/Red) based on Hoechst 33342 for live cells and propidium iodide nucleic acid stain for dead cells (Thermo Fischer Scientific). Cell viability was determined as the percentage of live cells among the total cells counted in six fluorescence images of each sample under a laser confocal microscope (LSM700 or LSM900; Carl Zeiss).

RNA-seq and data analysis

RNA-seq analysis was performed as previously described[81] with certain modifications. Total retinal RNAs from three *Otud7b*$^{+/+}$ and three *Otud7b*$^{-/-}$ mice after light exposure were isolated using TRIzol RNA extraction reagent (Invitrogen). Sequencing was performed on an Illumina NovaSeq 6000 platform in 101-base single-end mode. Raw reads were mapped to mouse reference genome sequences (mm10) using TopHat ver. 2.1.1, in combination with Bowtie2 ver. 2.2.8 and SAMtools ver. 0.1.18. The number of fragments per kilobase of exon per million mapped fragments (FPKMs) was calculated using Cuffdiff ver. 2.2.1. Upstream regulator analysis was performed using IPA (Qiagen). The RNA-seq analysis datasets are available in the Gene Expression Omnibus (GEO) database of NCBI (Accession Number GSE239573).

Luciferase reporter assay

Reporter gene assays were performed using the Nano-Glo Dual-Luciferase Reporter Assay System (Promega), according to the manufacturer's protocol. To generate the reporter construct, a minimal promoter (5′-AGACACTAGAGGGTATATAATGGAAGCTCGACTTCCAG-3′) and 5x NF-κB response element (5′-GGGAATTTCCGGGGACTTTCCGGGAATTTCCGGGGACTTTCCGGGAATTTCC-3′) were cloned into the pGL3-Basic vector (Promega) in which *Firefly luciferase* was replaced with *NanoLuc luciferase* amplified from the pNLF-N [CMV/Hygro] vector (Promega) by PCR. The pGL3-Basic vector containing the minimal promoter was co-transfected to measure transfection efficiency. A plasmid expressing Otud7b-shRNA1 was transfected with the reporter construct into Neuro2A cells. After 48 h of transfection, the cells were incubated in the serum-free medium for 14 h, washed with TBS, and lysed with buffer A. Luminescence signal was detected using the GloMax Multi+ Detection System (Promega).

QUANTIFICATION AND STATISTICAL ANALYSIS

Statistical analyses were performed using GraphPad Prism version 9 (GraphPad Software). Data are represented as the mean ± SD. Statistical analyses were performed using unpaired t-test, one-way ANOVA, or two-way ANOVA, as indicated in the figure legends. Asterisks indicate significance as follows: *$p < 0.05$, **$p < 0.01$, ***$p < 0.001$, and ****$p < 0.0001$.